

INTRAMOLECULAR C-C COUPLING REACTIONS OF ALKYNYL , VINYLIDENE AND ALKENYLPHOSPHANE LIGANDS IN RHODIUM (III) COMPLEXES

Sara Martínez de Salinas, Josefina Díez, Javier González, M. Pilar Gamasa and Elena Lastra*

Departamento de Química Orgánica e Inorgánica. Universidad de Oviedo. Julian Claveria, 8, 33006 Oviedo, Spain.

Supporting Information Placeholder

ABSTRACT: Electrophilic attack with methyl trifluoromethane sulfonate or tetrafluoroboric acid, to new alkynyl rhodium complexes containing alkenylphosphanes, lead to butenyne coupling products or to the unprecedented rhodaphosphacycle complexes $[\text{Rh}(\eta^5\text{-C}_5\text{Me}_5)\{\kappa^4\text{-}(P,C,C,C)\text{-iPr}_2\text{PCH}_2\text{C}(=\text{CH}_2)\text{C}(\text{CH}_2\text{R})\text{C}=\text{C}(\text{R})\}][\text{BF}_4]$ R = Ph (**11a**), *p*-tol (**11b**). These complexes **11a,b** can be explained as a result of the coupling of three organic fragments in the molecule, the alkynyl, the vinylidene, generated *in situ* by reaction with HBF_4 (**A**), and the C-C double bond from the alkenyl phosphane. DFT theoretical calculations on the formation of complex **11a** suggest the [2+2] intramolecular cycloaddition between the double bond of the allylphosphane and the $\text{C}\alpha\text{-C}\beta$ of the vinylidene **A**, as the most plausible pathway for this reaction.

INTRODUCCION

Inter- and intra-molecular reactions between alkynes and other organic fragments, promoted by transition metal complexes, have been the subject of active research in the last years, since they are among the most efficient and selective method for C-C bond formation¹ leading to a variety of organic compounds such as conjugated alkenes, α,β unsaturated aldehydes and ketones, enynes and others.²

In most of these reactions, the key organometallic species involved are alkynyl and/or vinylidene complexes. For example, the intramolecular coupling between alkynyl and vinylidene complexes leading to butenyne complexes is a key step in the alkyne dimerization, and therefore, the chemistry of these metallic complexes has been widely studied.³

On the other hand, alkenyl phosphanes bearing carbon-carbon double bonds display a versatile behavior as ligands in coordination chemistry and provide a double bond in the coordination sphere of the metals which can participate in coupling processes.

Kirchner and co-workers have studied the reactions of terminal and internal alkynes with Cp or Tp ruthenium complexes bearing alkenyl phosphanes which give rise to interesting coupling products resulting from the oxidative coupling between the olefin from the alkenyl phosphane and the alkyne.⁴ A similar behavior occurs when Cp ruthenium complexes were treated with propargyl alcohols obtaining dienyphosphane ligands.⁵ Also, the reactivity of Cp osmium complexes bearing alkenylphosphanes towards alkynes, has been widely studied by Esteruelas et al.⁶

Alkenylphosphane metal complexes are also involved in [2+2] cycloaddition reactions. Thus, the treatment of indenyl ruthenium(II) complexes bearing a bidentate ADPP ligand, with an excess of the corresponding terminal alkyne or propargylic alcohols lead diastereoselectively to bicyclic cyclobutylidene complexes through an intramolecular [2 + 2] cycloaddition between the C-C double bond of the alkenyl phosphane and the $\text{C}\alpha\text{-C}\beta$ of the vinylidene or allenylidene previously formed.⁷

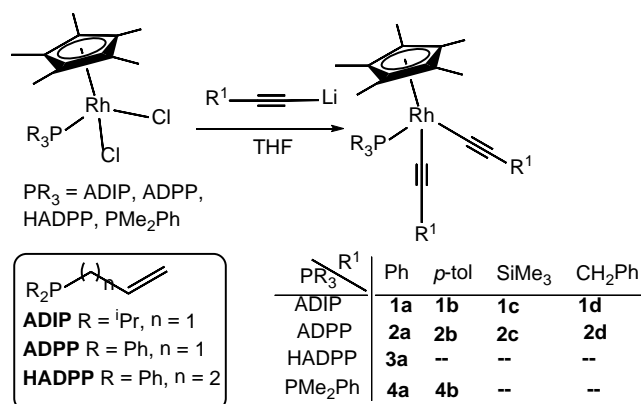
To explore the scope of these processes, we have investigated the behaviour of pentamethylcyclopentadienyl rhodium complexes with alkenylphosphanes allyldiiso-

propylphosphane (ADIP), allyldiphenylphosphane (ADPP) and homoallyldiphenylphosphane (HADPP) towards alkynes. For comparative purposes, complexes with PMe_2Ph have been also prepared.

RESULTS AND DISCUSSION

Synthesis of dialkynyl complexes. Complexes $[\text{RhCl}_2(\eta^5\text{-C}_5\text{Me}_5)\{\kappa^1(P)\text{-PR}_3\}]$ bearing the alkenyl phosphanes ADPP,⁸ ADIP,⁹ and HADPP⁹ react with 5 equivalents of freshly prepared solutions of lithium alkynyls to give the new dialkynyl rhodium complexes $[\text{Rh}(\eta^5\text{-C}_5\text{Me}_5)(\text{C}\equiv\text{CR}^1)_2\{\kappa^1(P)\text{-R}'_2\text{P}(\text{CH}_2)_n\text{CH}=\text{CH}_2\}]$ [$\text{R}' = \text{iPr}$, $n=1$, $\text{R}' = \text{Ph}$ (**1a**), $p\text{-tol}$ (**1b**), SiMe_3 (**1c**), CH_2Ph (**1d**); $\text{R}' = \text{Ph}$, $n=1$, $\text{R}' = \text{Ph}$ (**2a**), $p\text{-tol}$ (**2b**), SiMe_3 (**2c**), CH_2Ph (**2d**); $\text{R}' = \text{Ph}$, $n=2$, $\text{R}' = \text{Ph}$ (**3a**)] (Scheme 1). Also, the preparation of complexes bearing the phosphane PMe_2Ph $[\text{Rh}(\eta^5\text{-C}_5\text{Me}_5)(\text{C}\equiv\text{CR}^1)_2(\text{PPh}_2\text{Me})]$ ($\text{R}' = \text{Ph}$ (**4a**); $p\text{-tol}$ (**4b**)) have been accomplished for comparison purposes from $[\text{RhCl}_2(\eta^5\text{-C}_5\text{Me}_5)(\text{PMe}_2\text{Ph})]$ ¹⁰ (Scheme 1).¹¹

Scheme 1. Synthesis of dialkynyl rhodium(III) complexes.

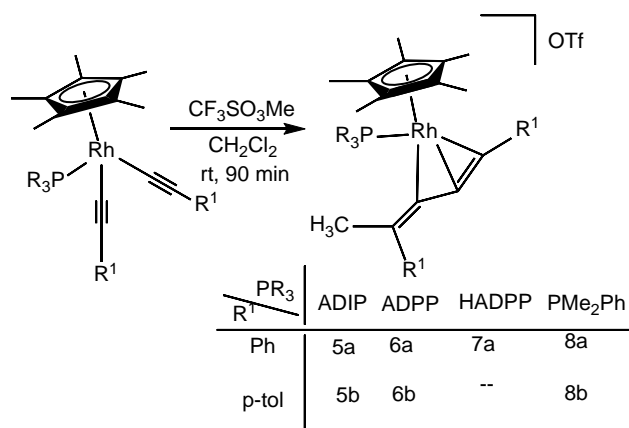


All complexes are stable yellow-brown solids or oils which have been analytically and spectroscopically characterized.^{11,12} Characteristic features of the spectroscopic data for these complexes are the following: (i) The IR spectra show the $\nu(\text{C}\equiv\text{C})$ absorption in the range 2028–2121 cm^{-1} ; (ii) the $^3\text{P}\{^1\text{H}\}$ NMR spectra in dichloromethane show a doublet for the phosphane ligand with coupling constants $^1J_{\text{RhP}}$ in the range 124.8–128.1 Hz as expected for coupling constants phosphorous-Rh(III). The chemical shifts observed for these complexes agree with a coordination $\kappa^1(P)$ of the alkenyl phosphanes [49.2–50.9 (ADIP), 39.5–41.2 (ADPP), 38.4 (HADPP) and 33.0–33.1 (PMe_2Ph)]; (iii) the ^1H and $^{13}\text{C}\{^1\text{H}\}$ NMR spectra show the expected signals for the C_5Me_5 and the phosphane ligands; (iv) the $^{13}\text{C}\{^1\text{H}\}$ NMR spectra of these complexes display characteristic resonances for the alkynyl groups: C_α as a doublet of doublets with coupling constants $^1J_{\text{CRh}}$ and $^2J_{\text{CP}}$ in the ranges 50.3–54.3 Hz and 27.2–34.2 Hz, respectively, and C_β atom as a doublet with $^2J_{\text{CRh}}$ in the range 6.1–13.1 Hz.

Reaction of dialkynyl complexes with methyl triflate. When the dialkynyl complexes **1a,b**, **2a,b**, **3a** and

4a,b are treated with methyl trifluoromethane sulfonate, the complexes **5a,b**, **6a,b**, **7a** and **8a,b**, containing a η^3 -butenylnyl group were formed (Scheme 2).

Scheme 2. Reaction of dialkynyl rhodium(III) complexes with $\text{CF}_3\text{SO}_3\text{Me}$.



Analytically pure samples of these complexes were obtained by anion exchange using NaBPh_4 salt (see experimental section for details). Also, these complexes have been completely characterized in solution by nuclear magnetic resonance spectroscopy including 1D and 2D NMR experiments (COSY, HSQC, HMBC and ROESY) and decoupling experiments [$^1\text{H}\{^3\text{P}\}$ and $^{13}\text{C}\{^3\text{P}\}\{^1\text{H}\}$]. In particular, it must be noted that (i) the $^3\text{P}\{^1\text{H}\}$ NMR spectra in dichloromethane show a doublet shifted toward higher field with respect to the corresponding precursors. The coupling constants phosphorous-Rh(III) ($^1J_{\text{RhP}}$) are in the range 155.7–162.8 Hz; (ii) the ^1H NMR spectra show the signals for the methyl group as a singlet in the range 2.46–2.78; (iii) The signals for the butenylnyl group in the $^{13}\text{C}\{^1\text{H}\}$ NMR spectra (Scheme 3, Table 1) agree with those found for other η^3 -butenylnyl complexes.¹³

Scheme 3. Carbon atom labels for the butenylnyl ligands

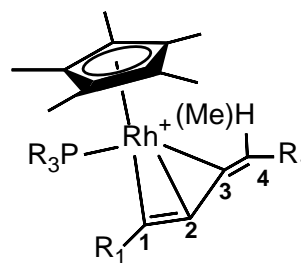


Table 1. $^{13}\text{C}\{^1\text{H}\}$ NMR data for complexes **5a,b**, **6a,b**, **7a** and **8a,b**.^[a]

	C-1	C-2	C-3	C-4
5a^b	109.8 (dd, $^1J_{\text{CRh}} = 14.1$, $^2J_{\text{CP}} = 5.0$)	44.6 (d, $^1J_{\text{CRh}} = 4.1$)	141.6 (dd, $^1J_{\text{CRh}} = 23.1$, $^2J_{\text{CP}} = 11.1$)	134.8
5b^b	109.7 (m)	43.1 s	140.6 (dd, $^1J_{\text{CRh}} = 21.1$, $^2J_{\text{CP}} = 11.1$)	130.9
6a^c	109.8 (d, $^1J_{\text{CRh}} = 11.1$)	44.5 s	142.6 (dd, $^1J_{\text{CRh}} = 23.1$, $^2J_{\text{CP}} = 9.7$)	135.0
6b^b	109.1 (dd, $^1J_{\text{CRh}} = 12.6$, $^2J_{\text{CP}} = 4.5$)	43.0 s	141.4 (dd, $^1J_{\text{CRh}} = 23.0$, $^2J_{\text{CP}} = 11.0$)	132.3
7a^b	109.8 (dd, $^1J_{\text{CRh}} = 11.8$, $^2J_{\text{CP}} = 3.6$)	43.8 s	142.8 (dd, $^1J_{\text{CRh}} = 22.4$, $^2J_{\text{CP}} = 10.9$)	134.3
8a^c	109.6 (dd, $^1J_{\text{CRh}} = 11.7$, $^2J_{\text{CP}} = 3.5$)	44.6 s	143.3 (dd, $^1J_{\text{CRh}} = 22.4$, $^2J_{\text{CP}} = 10.7$)	134.2
8b^c	109.4 (dd, $^1J_{\text{CRh}} = 11.6$, $^2J_{\text{CP}} = 2.7$)	43.7 s	142.2 (dd, $^1J_{\text{CRh}} = 23.0$, $^2J_{\text{CP}} = 11.0$)	133.5

[a] Chemical shift in ppm, coupling constants in Hz. [b] CD_2Cl_2 , 298K. [c] CD_2Cl_2 , 243K.

The structure of complex $[\text{Rh}(\eta^5\text{-C}_5\text{Me}_5)\{\eta^3\text{-CPh=C-C(=C(Ph)CH}_3)\}\{\kappa^1\text{-}(P)\text{-}i\text{Pr}_2\text{PCH}_2\text{CH=CH}_2\}][\text{CF}_3\text{SO}_3]$ (**5a**) was determined by single crystal X ray diffraction analysis. Slow diffusion of heptane into a solution of **5a** in dichloromethane, allowed us to collect suitable crystals for X-ray diffraction studies. An ORTEP type representation of the cation of complex **5a** is shown in Figure 1 and selected bonding data are collected in the caption.

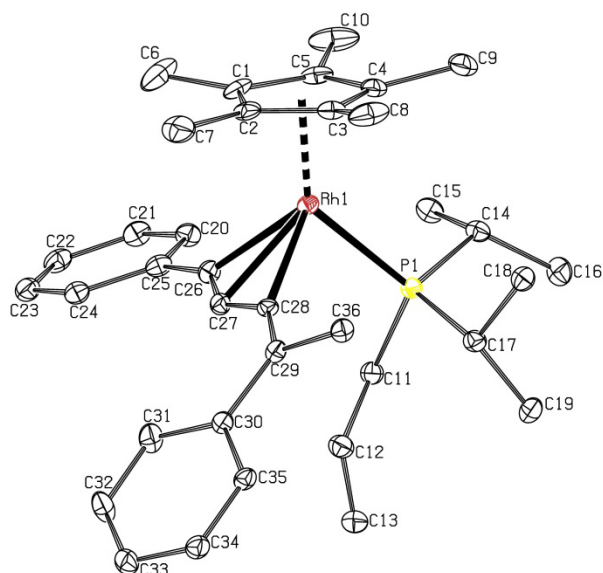


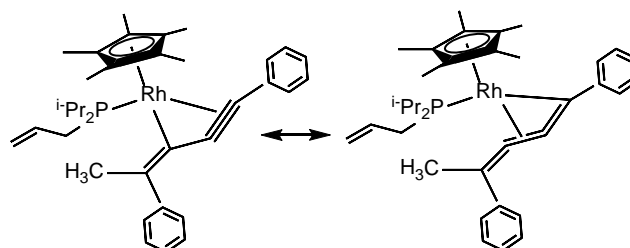
Figure 1. Molecular structure and atom-labeling scheme for the cation of complex $[\text{Rh}(\eta^5\text{-C}_5\text{Me}_5)\{\eta^3\text{-PC}_3\text{=C(Ph)CH}_3\}\{\kappa^1\text{-}(P)\text{-}i\text{Pr}_2\text{PCH}_2\text{CH=CH}_2\}][\text{CF}_3\text{SO}_3]$ (**5a**). Hydrogen atoms have been omitted for clarity. Non-hydrogen atoms are represented by their 20% probability ellipsoids. Selected bond lengths (Å): Rh(1)–P(1) = 2.354(1), Rh(1)–C* = 1.865(1), Rh(1)–C(26) = 2.252(3), Rh(1)–C(27) = 2.166(5), Rh(1)–C(28) = 2.130(4), C(12)–C(13) = 1.313(7), C(25)–C(26) = 1.460(7), C(26)–C(27) = 1.259(7), C(27)–C(28) = 1.365(7), C(28)–C(29) = 1.344(7), C(29)–C(30) = 1.481(7). Selected bond angles (deg): C*–Rh(1)–P(1) = 134.24(3), C*–Rh(1)–C(26) = 123.64(12), C*–Rh(1)–C(27) = 133.27(13), C*–Rh(1)–C(28) = 127.87(12), C(26)–Rh(1)–C(27) = 69.8(3), C(27)–Rh(1)–C(28) = 70.0(3), C(28)–Rh(1)–P(1) = 88.11(12), C(26)–Rh(1)–P(1) = 92.37(13), C(25)–C(26)–C(27) = 147.8(5), C(26)–C(27)–C(28) = 146.8(5),

C(27)–C(28)–C(29) = 140.3(5), C(28)–C(29)–C(30) = 121.5(4). C* = centroid of C(1), C(2), C(3), C(4), C(5).

The molecule exhibits a three-legged piano-stool geometry with the rhodium atom bonded to the phosphorus atom of the alkenylphosphane, η^5 - to the C_5Me_5 ligand, and η^3 to the 1,4-diphenyl-4-methylbut-3-en-1-ynyl ligand which exhibits an *E* stereochemistry.

The distances between Rhodium and C(26), C(27) and C(28) (2.130–2.252 Å) agree with the carbonated skeleton bonded η^3 . The C(27)–C(28) bond distance (1.365(7)) is similar to those in η^3 -allyl complexes and the C(26)–C(27) bond distance (1.259(7)) is in the range of carbon-carbon triple bond lengths in π -acetylene complexes. The angles C(25)–C(26)–C(27), C(26)–C(27)–C(28) and C(27)–C(28)–C(29) are 147.8(5), 146.8(5) and 140.3(5), respectively suggesting hybridization intermediate between sp and sp^2 for C(26), C(27) and C(28) atoms. Moreover, the C(25)–C(26) and C(29)–C(30) bond distances are intermediate between a single and double C–C bond, indicating an electronic delocalization through the aromatic rings. Thus, the topology of the butenynyl ligand in complex **5a** is similar to that observed in related complexes^{13,14} and its structure can be described as a combination of propargyl and allenyl resonance forms (Scheme 4).

Scheme 4. Resonance forms for butenynyl group in complex **5a**

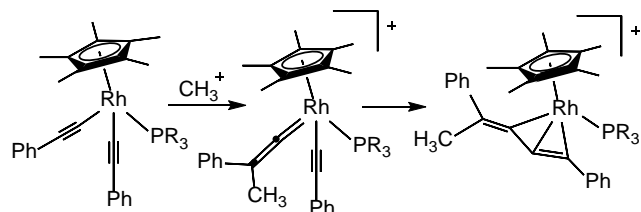


The crystal for the structure determination of complex **5a** belongs to the chiral space group $P2_12_12_1$, and the Flack parameter (-0.019(7)) indicates that a sole enantiomer is present in the asymmetric unit due to a spontaneous resolution on crystallization. An explanation for this fact

can be the separation of a conglomerate of enantiomorphous crystals of the two enantiomers upon crystallization from the racemic mixture. This spontaneous separation of one chiral crystalline form from a racemate solution has been occasionally observed.¹⁵

The formation of the butenynyl complexes can be explained through an intramolecular coupling of one alkynyl ligand with a transient vinylidene specie generated "in situ" by methylation of the second alkynyl unit (Scheme 5).¹⁶

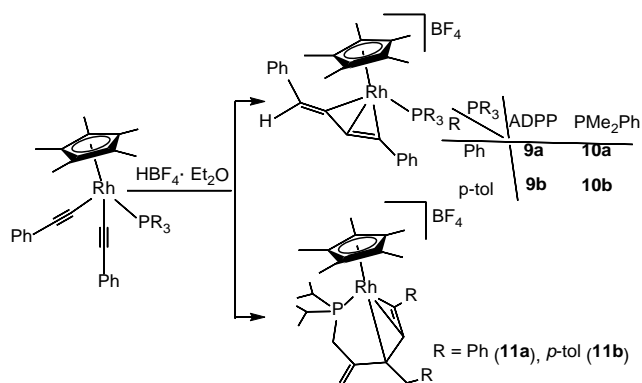
Scheme 5. Pathway for the formation of η^3 -dienyl complexes 5a,b, 6a,b, 7a and 8a,b.



The reaction of complexes **1c,d** and **2c,d** with methyl triflate lead to untractable reaction mixtures. Probably electronic delocalization of the butenynyl chain with the aromatic ring is necessary for stabilizing the products.

Reaction of dialkynyl complexes with tetrafluoroboric acid. When the dialkynyl complexes were treated with tetrafluoroboric acid, two different complexes can be isolated depending on the precursor. Thus, η^3 coordinated butenynyl complexes $[\text{Rh}(\eta^5\text{-C}_5\text{Me}_5)\{\eta^3\text{-CPh=C-C(=CHPh)}\}(\text{PR}_3)][\text{BF}_4]$ **9a,b** and **10a,b**, analogous to the former methylated complexes, were isolated (Scheme 5) for complexes **2a,b** and **4a,b**, containing the phosphanes ADPP and PMe_2Ph . Surprisingly, when complexes **1a,b** containing the ADIP phosphane, react with $\text{HBF}_4\cdot\text{OEt}_2$ in the same conditions, the unexpected and unprecedented rhodaphosphacycle complexes $[\text{Rh}(\eta^5\text{-C}_5\text{Me}_5)\{\kappa^4\text{-}(P,C,C,C)\text{-}^i\text{Pr}_2\text{PCH}_2\text{C(=CH}_2\text{)C(CH}_2\text{R)C=C(R)}\}][\text{BF}_4]$ **11a**, *p*-tol (**11b**) were obtained, resulting from the coupling of the three organic fragments in the molecule, the alkynyl, the vinylidene, generated *in situ* by reaction with HBF_4 , and the C-C double bond from the alkenyl phosphane (Scheme 6).

Scheme 6. Reaction of dialkynyl rhodium(III) complexes with tetrafluoroboric acid.



All complexes were isolated as stable solids and fully characterized by analytical and spectroscopic methods. Bidimensional (COSY, HSQC and HMBC) and decoupling NMR experiments have been carried out for the full assignment of the signals. Selected spectroscopic data for complexes **9a,b** and **10a,b** are the following: (i) The $^3\text{P}\{^1\text{H}\}$ NMR spectra show a doublet in the range expected for the coordinated phosphanes with coupling constants according with the existence of Rh(III) ($J_{\text{PRh}} = 160.3\text{-}162.1$ Hz); (ii) the ^1H NMR spectra show the signals for the hydrogen of the butenynyl fragment as a singlet at 7.12 (**9a,b**), 7.05 (**10a**) and 7.08 (**10b**) ppm; (iii) The signals for the butenynyl group in the $^{13}\text{C}\{^1\text{H}\}$ NMR spectra (Table 2), agree with those found for complexes **5a,b**, **6a,b**, **7a,b** and **8a,b**.

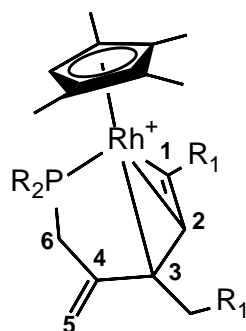
Table 2. $^{13}\text{C}\{^1\text{H}\}$ NMR data for complexes **9a,b** and **10a,b**.^[a]

	C-1	C-2	C-3	C-4
9a^b	117.2 (dd, $^1J_{\text{CRh}} = 14.1$, $^2J_{\text{CP}} = 4.0$)	42.4 (s)	142.8 (dd, $^1J_{\text{CRh}} = 21.1$, $^2J_{\text{CP}} = 8.0$)	124.7
9b^b	118.5 (m)	43.2 (s)	143.3 (dd, $^1J_{\text{CRh}} = 20.1$, $^2J_{\text{CP}} = 9.1$)	124.5
10a^c	117.0 (dd, $^1J_{\text{CRh}} = 14.1$, $^2J_{\text{CP}} = 3.6$)	41.5 (s)	141.6 (dd, $^1J_{\text{CRh}} = 20.1$, $^2J_{\text{CP}} = 4.0$)	123.8
10b^c	118.0 (dd, $^1J_{\text{CRh}} = 15.1$, $^2J_{\text{CP}} = 4.1$)	42.4 (s)	142.1 (dd, $^1J_{\text{CRh}} = 21.1$, $^2J_{\text{CP}} = 9.1$)	123.7

[a] Chemical shift in ppm, coupling constants in Hz. [b] CD_2Cl_2 , 243K. [c] CD_2Cl_2 , 298K.

Characteristic features of the spectroscopic data for complexes **11a,b** are the following: (i) IR show the characteristic broad band for the BF_4 anion at 1032 (**11a**) and 1051 (**11b**) cm^{-1} ; (ii) the $^3\text{P}\{^1\text{H}\}$ NMR spectra in dichloromethane show a doublet at 54.1 ($^1J_{\text{RhP}} = 157.3$) (**11a**) and 53.8 ($^1J_{\text{RhP}} = 156.7$) (**11b**) ppm; (iii) the ^1H and $^{13}\text{C}\{^1\text{H}\}$ NMR spectra show the signals for the 7-membered rodaphosphacycle (Table 3, Scheme 7).

Scheme 7. Carbon atom labels for the butenylnyl ligands

**Table 3.** $^{13}\text{C}\{^1\text{H}\}$ NMR data for complexes **11a,b**.^[a, b]

	11a	11b
C-1	92.7 (dd, $^1J_{\text{CRh}} = 17.1$, $^2J_{\text{CP}} = 5.0$)	92.7 (dd, $^1J_{\text{CRh}} = 16.1$, $^2J_{\text{CP}} = 4.0$)
C-2	80.4 (d, $^1J_{\text{CRh}} = 2.0$)	79.5 (s)
C-3	83.6 (dd, $^1J_{\text{CRh}} = 8.0$, $^2J_{\text{CP}} = 2.0$)	83.7 (d, $^1J_{\text{CRh}} = 7.0$)
C-4	142.6 (d, $^2J_{\text{CP}} = 1.0$)	142.9 (s)
C-5	115.8 (d, $^3J_{\text{CP}} = 11.1$)	115.5 (d, $^3J_{\text{CP}} = 12.1$)
C-6	25.3 (d, $^1J_{\text{CP}} = 24.1$)	25.3 (d, $^1J_{\text{CP}} = 24.1$)

[a] Chemical shift in ppm, coupling constants in Hz. [b] CD_2Cl_2 , 298K.

Slow diffusion of heptane into a solution of complex **11a** in a mixture dichloromethane/diethylether at room temperature allows crystals suitable for X-ray diffraction studies. For complex **11a**, the asymmetric unit consists of two molecules. For one of them, the rodaphosphacycle chain is disordered at 50% into two different positions. However in the second molecule, the rodaphosphacycle

chain is located in only one position. In the present paper, only this molecule is presented and discussed, since the more relevant structural parameters are similar in both molecules. ORTEP type representation of the cation is shown in Figure 2 and selected bonding data are collected in the caption.

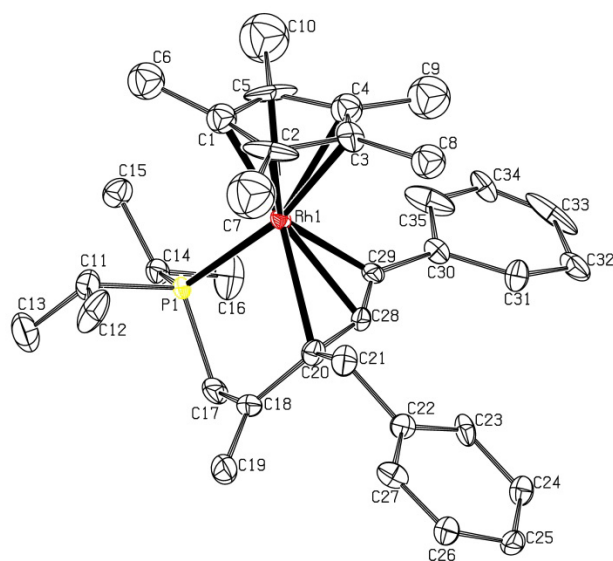


Figure 2. Molecular structure and atom-labeling scheme for the cation of complex $[\text{Rh}(\eta^5\text{-C}_5\text{Me}_5)\{\kappa^4\text{-}(P,C,C,C)\text{-}^i\text{Pr}_2\text{PCH}_2\text{C}(\text{=CH}_2)\text{C}(\text{CH}_2\text{Ph})\text{C}(\text{=C}(\text{Ph}))\}][\text{BF}_4]$ **11a**. Hydrogen atoms have been omitted for clarity. Non-hydrogen atoms are represented by their 10% probability ellipsoids. Selected bond lengths (\AA): $\text{Rh}(1)\text{-P}(1) = 2.324(2)$, $\text{Rh}(1)\text{-C}^* = 1.848(11)$, $\text{Rh}(1)\text{-C}(20) = 2.424(15)$, $\text{Rh}(1)\text{-C}(28) = 2.222(12)$, $\text{Rh}(1)\text{-C}(29) = 2.165(17)$, $\text{P}(1)\text{-C}(17) = 1.777(17)$, $\text{C}(17)\text{-C}(18) = 1.48(3)$, $\text{C}(18)\text{-C}(19) = 1.40(3)$, $\text{C}(18)\text{-C}(20) = 1.48(2)$, $\text{C}(20)\text{-C}(21) = 1.54(2)$, $\text{C}(21)\text{-C}(22) = 1.51(2)$, $\text{C}(20)\text{-C}(28) = 1.40(2)$, $\text{C}(28)\text{-C}(29) = 1.14(2)$, $\text{C}(29)\text{-C}(30) = 1.59(2)$. Selected bond angles (deg): $\text{C}^*\text{-Rh}(1)\text{-P}(1) = 136.79(9)$, $\text{C}^*\text{-Rh}(1)\text{-C}(20) = 135.1(6)$, $\text{C}^*\text{-Rh}(1)\text{-C}(28) = 134.2(3)$, $\text{C}^*\text{-Rh}(1)\text{-C}(29) = 122.6(5)$, $\text{P}(1)\text{-Rh}(1)\text{-C}(20) = 79.1(4)$, $\text{C}(20)\text{-Rh}(1)\text{-C}(28) = 34.7(5)$, $\text{C}(28)\text{-Rh}(1)\text{-C}(29) = 30.0(6)$, $\text{P}(1)\text{-Rh}(1)\text{-C}(29) = 93.6(3)$, $\text{P}(1)\text{-C}(17)\text{-C}(18) = 104.9(12)$, $\text{C}(17)\text{-C}(18)\text{-C}(19) = 120.3(17)$, $\text{C}(17)\text{-C}(18)\text{-C}(20) = 116.2(14)$, $\text{C}(18)\text{-C}(20)\text{-C}(28) = 118.6(13)$, $\text{C}(20)\text{-C}(28)\text{-C}(29) = 151.4(14)$, $\text{C}(28)\text{-C}(29)\text{-C}(30) = 140.2(14)$. C^* = centroid of C(1), C(2), C(3), C(4), C(5).

The molecule exhibits a three-legged piano-stool geometry with the rhodium atom bonded η^5 - to the C_5Me_5 ligand, to the phosphorus atom, and the C(20), C(28) and C(29) carbon atoms of the newly formed tetradentate ligand. The distances between the rhodium atom and C(20), C(28) and C(29) carbon atoms are 2.424(16),

2.222(12) and 2.165(17) Å, respectively and agree with a single Rh-C bond as found for complex **5a**. The C(20)-C(28) and C(28)-C(29) bond distances show an electronic delocalization through the three carbon atoms.

Computational Study. In order to get some insights about the mechanisms underlying the transformation of dialkynyl rhodium (III) complexes into the η^3 -dienyl complexes **5-10** or the rhodaphosphacycle complexes **11**, a theoretical study using the Density Functional theory, was carried out.¹⁷ Full details of the potential-energy surfaces studied, including a reaction-energy profile, are shown in the Supporting Information section.

As summarized in Scheme 6, the reaction of alkynyl complexes **1a,b** and **2a,b** with tetrafluoroboric acid leads to complexes **9ab-10ab** or to the complex **11a**, depending on the nature of the phosphine ligand. According to the calculations, for complex **1a**, the first step in these reactions appears to be the protonation of one alkynyl group, to form the cationic alkynylvinylidene complex **A** (Scheme 8). This reaction appears to occur without an appreciable energy barrier (after an extensive search, the corresponding transition state has not been located), the intermediate **A** being predicted to be 15 kcal mol⁻¹ more stable than the starting materials (**1a** + HBF₄). The posterior evolution of the cationic vinylidene intermediate depends on the structure of the phosphine. At first, it was found that the vinylidene **A** can undergo an intramolecular cyclization to give the η^3 -dienyl complex **12a** (Scheme 8), analogous to complexes **9a** and **10a**. In this reaction, a C-C bond is formed through the transition state **TS1** (Figure 3). The reaction product **12a** is predicted to be 35.2 kcal mol⁻¹ more stable than the reactants and the activation barrier is very low ($\Delta G^\ddagger = +3.6$ kcal mol⁻¹).

Scheme 8. Stationary points located for the mechanism of the formation of complex **12a** at low temperature. Energies are given in kcal mol⁻¹.

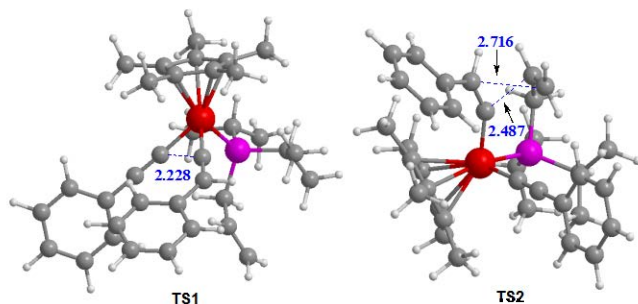
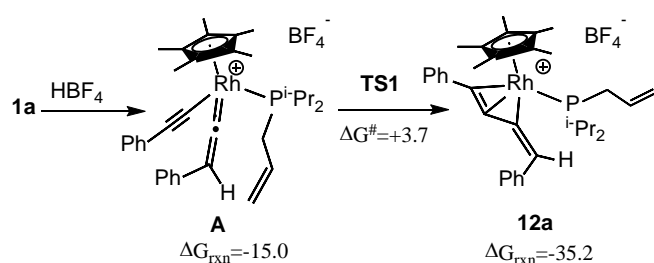
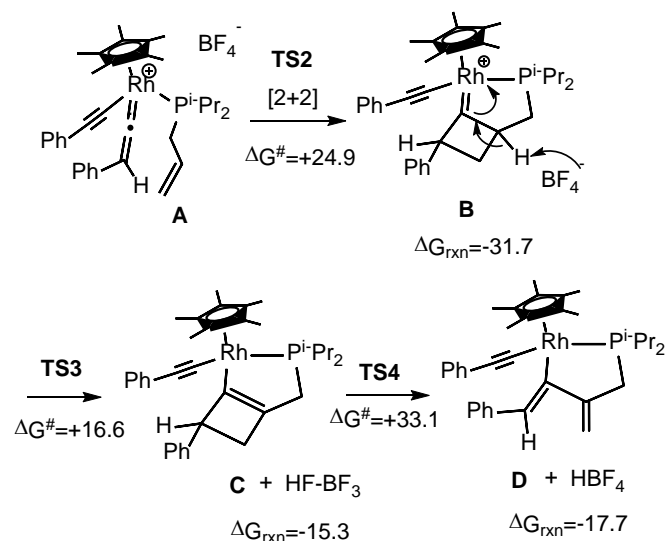


Figure 3. Transition states located for the cyclization (**TS1**) and [2+2] intramolecular cycloaddition (**TS2**) of vinylidene **A**. The tetrafluoroborate anion has been deleted for clarity. Lengths are in Å.

However, for compound **1a**, only the rhodaphosphacycle complex **11a** was isolated (Scheme 6), thus suggesting the possibility of compound **12a** being an intermediate in the formation of product **11a**. The found mechanism, leading to **11a** from **12a**, involves the formation of a phospharhodacyclobutane intermediate (see the Supporting Information for details) and it is predicted to have a high activation barrier (up to 58 kcal mol⁻¹), which is not compatible with the conditions of the reaction, and was ruled out.

At this point, other mechanism, without the participation of **12a** as intermediate, was studied. In this case, the transformation of **A** into **11a**, starts with the [2+2] intramolecular cycloaddition between the double bond of the allylphosphane and the C α -C β double bond of the vinylidene **A**, which leads to the bicycle **B** (Scheme 9). The calculated activation barrier for this process is 24.9 kcal mol⁻¹, and the reaction free energy is -16.7 kcal mol⁻¹.

Scheme 9. Intramolecular [2+2]-cycloaddition reaction of vinylidene **A**, followed by the deprotonation of the bicyclic adduct **B**, and the conrotatory ring opening of **C**, to give the diene derivative **D**. Energies are in kcal mol⁻¹.

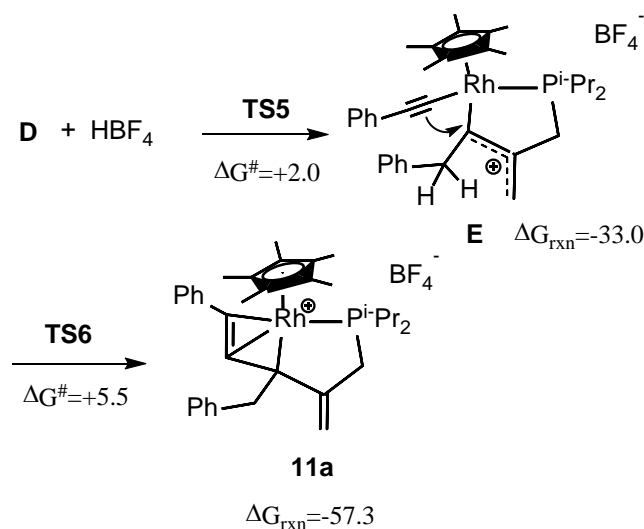


Some geometrical details of the transition state **TS2** are shown in Figure 3. The deprotonation of cyclobutylidene **B** leads to the cyclobutenyl derivative **C**, which could undergo a thermal, four-electrons conrotatory electrocyclic ring-opening (**TS4**, Figure 4), to give rise intermediate **D**, which is 2.4 kcal mol⁻¹ more stable than the cyclobutenyl **C**. [2+2] intramolecular cycloaddition reactions between the double bond of an allylphosphane and the C α -C β of a vinylidene leading to cyclobutylidene complexes have been recently reported for ruthenium complexes.^{7,18} Also, the deprotonation of these cyclobutenyli-

dene ring lead to cyclobutenyl complexes,^{7a} supporting the proposed pathway.

In Scheme 10, the final steps of the proposed mechanism are outlined. The protonation of the diene derivative **D** results in the formation of the allyl cationic intermediate **E**, which in turn, experiences the attack of the triple bond (TS6, Figure 4), thus leading to the final product **11a**. The final product **11a** is predicted to be a very stable compound, being the large negative value of ΔG_{rxn} the driving force of the full process.

Scheme 10. Protonation of diene D to give the allyl cation E, and intramolecular cyclization leading to final product 11a.



From the results shown, it appears that the protonation of **1a** should lead to the formation of two products, **11a** and **12a**. However, although product **12a** will be formed initially, due to the small activation barrier from vinylidene **A**, *e. g.* **12a** is the kinetic control product, the barrier for its reversion to **A** ($31.9 \text{ kcal mol}^{-1}$) is slightly lower than the barrier ($33.1 \text{ kcal mol}^{-1}$) for the ring opening of intermediate **C**, which is the rate-determining step in the formation of **11a**. Accordingly, the formation of **12a** is reversible, and in thermodynamic conditions, the only product detected will be the very stable rhodaphosphacycle complex **11a**.

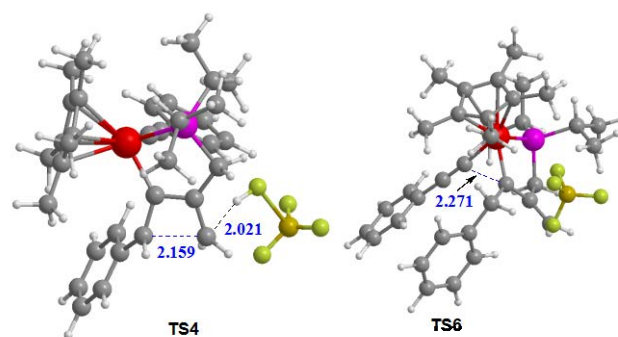
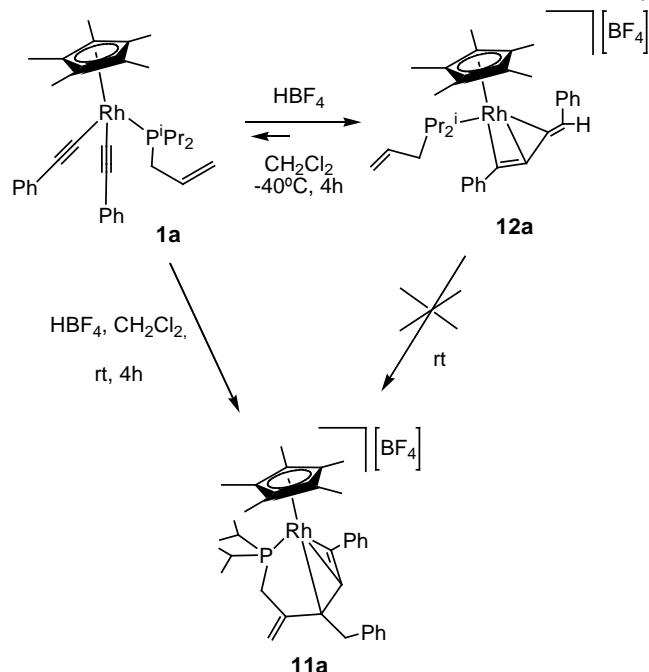


Figure 4. Transition states located for the conrotatory ring opening (**TS4**) of intermediate **C** and intramolecular cyclization (**TS6**) of allyl cation **E**. Lengths are in Å.

The formation of **12a** from the mixture of **1a** and HBF_4 was observed experimentally. Thus, the addition of tetrafluoroboric acid to complex **1a**, carried out at 233 K, was monitored by $^3\text{P}\{^1\text{H}\}$ and $^{13}\text{C}\{^1\text{H}\}$ NMR. The formation of a transient specie is assessed by the $^3\text{P}\{^1\text{H}\}$ NMR spectrum of the reaction mixture, which shows, after 4 h at low temperature, a doublet resonance at $\delta = 41.4 \text{ ppm}$ ($J_{\text{PRh}} = 155.8 \text{ Hz}$). Also, the $^{13}\text{C}\{^1\text{H}\}$ NMR spectrum agree with the formation in solution of a butenynyl complex $[\text{Rh}(\eta^3\text{-C}_3\text{Me}_3)\{\eta^3\text{-CPh=C-C(=CHPh)}\}\{\kappa^1\text{-}(P)\text{-}^i\text{Pr}_2\text{PCH}_2\text{CH=CH}_2\}][\text{BF}_4]$ (**12a**), analogous to complexes **9a** and **10a**, since presents two singlets at $\delta = 43.9, 123.6$ and two multiplets at $\delta = 118.5$ and 142.8 for C-2, C-4, C-1 and C-3 carbon atoms, respectively. Complex **12a** is unstable at room temperature and all isolation attempts were unsuccessful. These studies shown that **12a** is not an intermediate in the formation of **11a**, but a parallel product, that being unstable at room temperature, could not be isolated (Scheme 11).

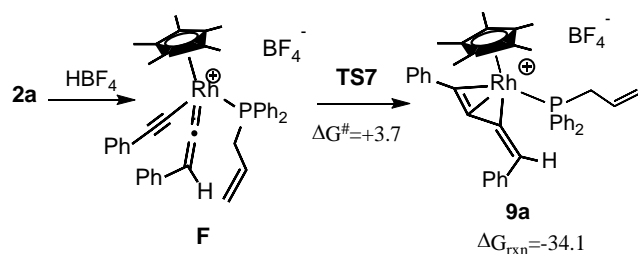
Scheme 11. Reaction of complex 1a with HBF₄



The results shown in Scheme 6 indicate that the nature of the phosphine ligand strongly influences the course of the reaction of dialkynyl rhodium (III) complexes with tetrafluoroboric acid. When the reaction is carried out with complex **2a**, bearing the allyldiphenylphosphine ligand, only the η^3 -dienyl complex **9a** is formed, and not trace of the rhodaphosphacycle complex is detected, in sharp contrast with the case of the allyldiisopropylphosphine-bearing dialkynyl rhodium complex **1a**. In order to understand the reason of this unexpected behaviour, the intramolecular cyclization reaction of the cationic vinylidene intermediate **F** (Scheme 12), which is considered to form upon protonation of **2a**, was studied.

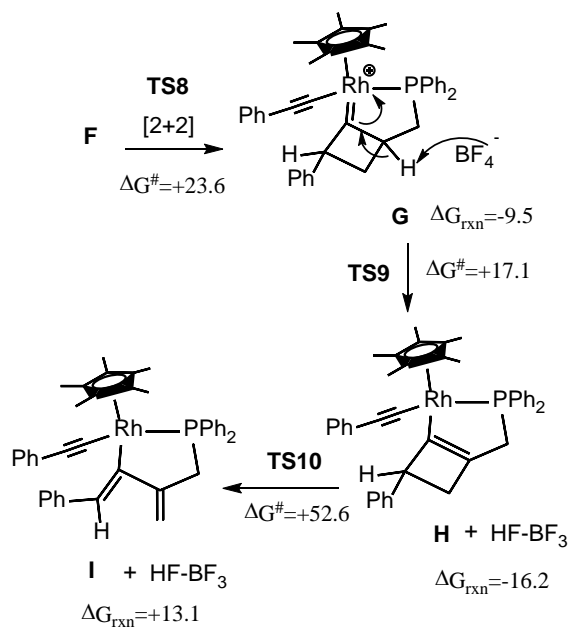
Intermediate **F** was found to experience the intramolecular cyclization leading to complex **9a**, in a reaction with a small barrier, in good agreement with the experimental data. The values of ΔG^\ddagger and ΔG_{rxn} for this reaction are similar to those found for the case of the vinylidene **A** (see Scheme 8), which is reasonable, taking into account the close relationship between both reactions.

Scheme 12. Reaction of complex 2a with HBF₄. Energies are in kcal mol⁻¹.



The fact that the reaction of complex **2a** do not leads to a rhodaphosphacycle complex, as it happens in the case of **1a**, could be explained assuming that some step in the corresponding mechanism, presents a high activation energy, thus inhibiting this reaction pathway. In this regard, it was found (Scheme 13) that, while the [2+2]-cycloaddition reaction of vinylidene intermediate **F** and the deprotonation reaction of cyclobutylidene **G** present values of ΔG^\ddagger and ΔG_{rxn} very close to those of the vinylidene **A**, the free-activation energy of the ring opening reaction of intermediate **H** is about 19 kcal mol⁻¹ higher than the free-activation energy of the reaction of the analogous intermediate **C**. In addition, the formation of the diene intermediate **I** is clearly exothermic, by 13.1 kcal mol⁻¹. Thus, it seems reasonable that in the case of the complex **2a**, the only viable reaction channel is the one leading to the η^3 -dienyl complex **9a**.

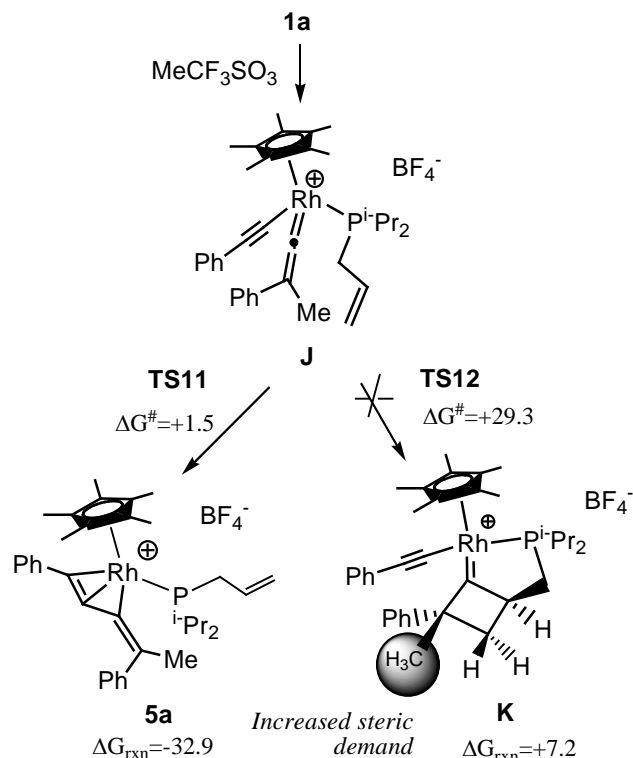
Scheme 13. Intramolecular [2+2]-cycloaddition of vinylidene F, deprotonation reaction of adduct G, and conrotatory ring opening of intermediate H, to give the diene derivative I. Energies are in kcal mol⁻¹.



The proposed mechanism also accounts for the different reactivity observed when complex **1a** reacts with methyl triflate (see Scheme 14). In this case, the isolated product is the η^3 -butenylnyl group-containing complex **5a**. The formation of this product can be explained by the low-barrier ($\Delta G^\ddagger = +1.5$ kcal mol⁻¹) for the intramolecular coupling of the alkynyl and the vinylidene fragments in the vinylidene intermediate **J** (see Supporting Information section for details), which is formed in the methylation of **1a**. According to the calculations, complex **5a** is predicted to be 32.9 Kcal mol⁻¹ more stable than intermediate **J**. On the other hand, the intramolecular [2+2] cycloaddition of the vinylidene to form a cyclobutylidene intermediate **K** presents an activation barrier which is 4.4 kcal mol⁻¹ higher than the analogous reaction of intermediate **A** ($\Delta G^\ddagger = +29.3$ kcal mol⁻¹). Also, the formation of this intermediate

is predicted to be endothermic by +7.2 kcal mol⁻¹. According to this result, **K** will not be formed, and the reaction does not progress towards a rhodaphosphacycle system analog to **11a**. Both, the high activation barrier for the [2+2] cycloaddition and the minor thermodynamic stability of cyclobutylidene **K**, reflect the greater steric demand of the methyl group, as compared with the hydrogen atom.

Scheme 14. Formation of complex 5a by intramolecular coupling of the alkynyl and vinylidene fragments in intermediate J.



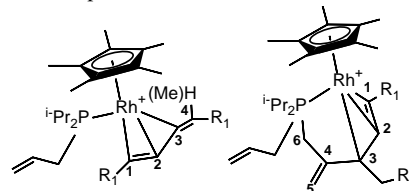
CONCLUSIONS

The alkynyl rhodium complexes [Rh(η⁵-C₅Me₅)(C≡CR)₂{κ¹-(P)-R'₂P(CH₂)_nCH=CH₂}] (**1a,b**, **2a,b**, **3a** and **4a,b**) react with methyl trifluoromethane sulfonate leading to butenylnyl coupling products. However, complexes **1c,d** and **2c,d** which present non-aromatic substituents in the alkynyl group react with methyl triflate to give untractable reaction mixtures, indicating that delocalization with the aromatic ring is necessary for stabilizing the products. Also, complexes [Rh(η⁵-C₅Me₅)(C≡CR)₂{κ¹-(P)-iPr₂PCH₂CH=CH₂}] (R = Ph, *p*-tol) react with tetrafluoroboric acid to generate the unprecedented complexes [Rh(η⁵-C₅Me₅){κ⁴-(P,C,C,C)-iPr₂PCH₂C(=CH₂)C(CH₂R)C=C(R)}][BF₄⁻] (R = Ph (**11a**), *p*-tol (**11b**), resulting from the coupling of the three organic fragments in the molecule. DFT theoretical calculations on the formation of complex **11a** suggest the [2+2] intramolecular cycloaddition between the double bond of the

alkenylphosphane and the Cα-Cβ of the vinylidene generated *in situ* by reaction with HBF₄ (**A**), as the most plausible pathway for this reaction. This pathway also accounts for the different reactivity observed in the reaction with methyl triflate to yield the η³-butenyl group-containing complex **5a** and the differences of reactivity found for complexes **1a** and **2a** bearing ADIP and ADPP, respectively.

EXPERIMENTAL SECTION

General Procedures. All manipulations were performed under an atmosphere of dry nitrogen using vacuum-line and standard Schlenk techniques. The reagents were obtained from commercial suppliers and used without further purification. Solvents were dried by standard methods and distilled under nitrogen before use. Complexes [RhCl₂(η⁵-C₅Me₅){κ¹-(P)-PR₃}] were prepared by previously reported procedures.⁸⁻¹⁰ Infrared spectra were recorded on a PerkinElmer 1720-XFT spectrometer. The C, H, and N analyses were carried out with a PerkinElmer 240-B and a LECO CHNS-TruSpec microanalyzer. Mass spectra (ESI) were determined with a Bruker Esquire 6000 spectrometer, operating in positive mode and using dichloromethane and methanol solutions. NMR spectra were recorded on Bruker spectrometers AV400 operating at 400.13 (1H), 100.61 (13C), and 161.95 (31P) MHz, AV300 operating at 300.13 (1H), 75.45 (13C), and 121.49 (31P) MHz, and AV600 operating at 600.15 (1H) MHz and 150.91 (13C) MHz. DEPT and 2D COSY HH, HSQC, and HMBC experiments were carried out for all the compounds. Chemical shifts are reported in parts per million and referenced to TMS or 85% H₃PO₄ as standards. Coupling constants J are given in hertz. Abbreviations used: s, singlet; d, doublet; dd, double doublet; t, triplet; sept, septuplet; m, multiplet. Experimental section includes a complete set of data for complexes bearing the phosphane ADIP (**1a-d**, **5a,b**, **8a,b**, **9a,b** and **11a,b**). The experimental data for complexes bearing phosphanes, ADPP, HADPP and PMe₂Ph are provided as Supporting Information. The following atom labels are used for the ¹³C{¹H} NMR spectroscopic data.



Synthesis of dialkynyl complexes [Rh(η⁵-C₅Me₅)(C≡CR)₂{κ¹-(P)-iPr₂PCH₂CH=CH₂}] (R = Ph (1a**), *p*-tol (**1b**)).** To a solution of the complex [Rh(η⁵-C₅Me₅)Cl₂{κ¹-(P)-iPr₂PCH₂CH=CH₂}] (200 mg, 0.43 mmol) in THF (20 mL) was added a solution of the correspondent lithium acetylide in THF freshly prepared by addition of 1.90 mmol of the corresponding alkyne and LiⁿBu). The resulting colored solution was stirred at room temperature for 15 min. Then, the solution was evaporated to dryness and the solid residue was treated with dichloromethane (25 ml) and filtered. Evaporation of the filtrate and the addition of diethyl ether (20 mL) yielded a yellow-brown solid which are dried under vacuum. R = Ph (**1a**), (0.13 g, 50%): ¹H NMR (400.1 MHz, CD₂Cl₂, 298K) δ = 1.30-1.47 (m, 12H, PCH(CH₃)₂), 1.93 (s, 15H, C₅Me₅), 2.40 (m, 2H, PCH(CH₃)₂), 3.30 (m, 2H, PCH₂), 5.13 (m, 2H, =CH₂), 6.23 (m, 1H, CH=CH₂), 7.15 (m, 2H, Ph), 7.28 (m, 4H, Ph), 7.36 (m, 4H, Ph) ppm; ¹³C {¹H} NMR (100.6 MHz, CD₂Cl₂, 298K) δ = 10.1 (s, CH₃, C₅Me₅), 18.7, 19.0 (2s, PCH(CH₃)₂), 26.9 (d, ¹J_{CP} = 22.1 Hz, PCH(CH₃)₂), 29.7 (d, ¹J_{CP} = 30.2 Hz, PCH₂), 101.0 (s, C₅Me₅), 103.6 (d, ³J_{CP} = 8.0 Hz, C_β), 105.1 (dd, ³J_{CP} = 30.2 Hz, ¹J_{CRH} = 54.3 Hz, C_α), 117.2 (d, ³J_{CP} = 9.1 Hz,

=CH₂), 124.3 (s, Ph), 127.8 (s, Ph), 129.5 (s, Ph), 130.7 (s, Ph), 134.1 (d, ²J_{CP} = 8.1 Hz, CH=CH₂) ppm; ³¹P {¹H} NMR (121.5 MHz, CD₂Cl₂, 298K) δ = 50.1 (d, ¹J_{RhP} = 124.8 Hz) ppm; IR (KBr): ν = 2097 (m, C≡C) cm⁻¹; MS (ESI): *m/z* 620 [M + Na]⁺, 462 [M + Na - ADIP]⁺; elemental analysis calc (%) for C₃₅H₄₄PRh · 1/2 CH₂Cl₂ (641.06): C 66.51, H 7.08; found: C 66.76, H 6.99. R = *p*-tol (**1b**), (0.20 g, 75%): ¹H NMR (400.1 MHz, CD₂Cl₂, 298K) δ = 1.20-1.45 (m, 12H, PCH(CH₃)₂), 1.95 (d, ⁴J_{HP} = 2.3 Hz, 15H, C₅Me₅), 2.15-2.50 (m, 8H, PCH(CH₃)₂), CH₃ *p*-tol, 3.39 (m, 2H, PCH₂), 5.13-5.24 (m, 2H, =CH₂), 6.30 (m, 1H, CH=CH₂), 7.05 (d, ³J_{HH} = 7.1 Hz, 2H, *p*-tol), 7.23 (d, ³J_{HH} = 8.1 Hz, 2H, *p*-tol) ppm; ¹³C {¹H} NMR (100.6 MHz, CD₂Cl₂, 298K) δ = 10.1 (s, CH₃, C₅Me₅), 18.7, 19.0 (2s, PCH(CH₃)₂), 20.9 (s, CH₃, *p*-tol), 26.9 (d, ¹J_{CP} = 22.2 Hz, PCH(CH₃)₂), 29.8 (d, ¹J_{CP} = 30.2 Hz, PCH₂), 100.8 (s, C₅Me₅), 103.3 (d, ³J_{CP} = 10.1 Hz, C_β), 103.3 (dd, ²J_{CP} = 30.1 Hz, ¹J_{CRh} = 53.3 Hz, C_α), 117.1 (d, ³J_{CP} = 9.1 Hz, =CH₂), 126.8 (s, *p*-tol), 128.5 (s, *p*-tol), 130.5 (s, *p*-tol), 131.3 (s, *p*-tol), 134.2 (d, ²J_{CP} = 8.1 Hz, CH=CH₂) ppm; ³¹P {¹H} NMR (121.5 MHz, CD₂Cl₂, 298K) δ = 50.9 (d, ¹J_{RhP} = 125.1 Hz) ppm; IR (KBr): ν = 2084 (s, C≡C) cm⁻¹; elemental analysis calc (%) for C₃₇H₄₈PRh (626.67): C 70.92, H 7.72; found: C 69.32, H 7.24.

Synthesis of complexes [Rh(η⁵-C₅Me₅)(C≡CR)₂{κ¹-(P)-Ph₂PCH₂CH=CH₂}] (R = Ph (2a**), *p*-tol (**2b**)).** To a solution of the complex [Rh(η⁵-C₅Me₅)Cl₂{κ¹-(P)-Ph₂PCH₂CH=CH₂}] (200 mg, 0.38 mmol) in THF (20 mL) was added a freshly solution of the correspondent lithium acetylide in THF (1.90 mmol, molar ratio Rh/Li = 1/5). The resulting colored solution was stirred at room temperature for 15 min. Then, the solution was evaporated to dryness and the solid residue was treated with dichloromethane (25 mL) and filtered. Evaporation of the filtrate and the addition of diethyl ether (20 mL) yielded a yellow solid which are dried under vacuum. R = Ph (**2a**), (0.13 g, 50%): ¹H NMR (400.1 MHz, CD₂Cl₂, 298K) δ = 1.62 (d, ⁴J_{HP} = 2.8 Hz, 15H, C₅Me₅), 3.81 (m, 2H, PCH₂), 4.78 (m, 1H, =CH₂), 4.88 (m, 1H, =CH₂), 5.84 (m, 1H, CH=CH₂), 7.12 (m, 2H, Ph), 7.21 (m, 4H, Ph), 7.32 (m, 4H, Ph), 7.49 (m, 6H, Ph), 7.88 (m, 4H, Ph) ppm; ¹³C {¹H} NMR (100.6 MHz, CD₂Cl₂, 298K) δ = 8.9 (s, CH₃, C₅Me₅), 36.8 (d, ¹J_{CP} = 34.2 Hz, PCH₂), 100.9 (s, C₅Me₅), 103.8 (d, ³J_{CP} = 10.6 Hz, C_β), 105.3 (dd, ²J_{CP} = 32.2 Hz, ¹J_{CRh} = 53.3 Hz, C_α), 118.3 (d, ³J_{CP} = 10.6 Hz, =CH₂), 124.5 (s, Ph), 127.7 (s, Ph), 127.8 (d, ³J_{CP} = 4.0 Hz, Ph), 129.2 (s, Ph), 130.2 (d, ¹J_{CP} = 33.0 Hz, Ph), 130.3 (s, Ph), 130.9 (s, Ph), 131.7 (d, ²J_{CP} = 10.6 Hz, CH=CH₂), 134.0 (d, ²J_{CP} = 9.0 Hz, Ph) ppm; ³¹P {¹H} NMR (121.5 MHz, CD₂Cl₂, 298K) δ = 40.4 (d, ¹J_{RhP} = 128.1 Hz) ppm; IR (KBr): ν = 2095 (m, C≡C) cm⁻¹; MS (ESI): *m/z* 689 [M + Na]⁺, 463 [M + Na - ADPP]⁺; elemental analysis calc (%) for C₄₁H₄₀PRh (666.65): C 73.87, H 6.05; found: C 73.24, H 5.96. R = *p*-tol (**2b**), (0.20 g, 76%): ¹H NMR (400.1 MHz, CD₂Cl₂, 298K) δ = 1.62 (d, ⁴J_{HP} = 3.0 Hz, 15H, C₅Me₅), 2.35 (s, 6H, CH₃), 3.81 (m, 2H, PCH₂), 4.69-4.76 (m, 1H, =CH₂), 4.80-4.90 (m, 1H, =CH₂), 5.83 (m, 1H, CH=CH₂), 7.05 (d, ³J_{HH} = 7.7 Hz, 2H, *p*-tol), 7.23 (d, ³J_{HH} = 7.9 Hz, 2H, *p*-tol), 7.49 (m, 6H, Ph), 7.90 (m, 4H, Ph) ppm; ¹³C {¹H} NMR (100.6 MHz, CD₂Cl₂, 298K) δ = 8.9 (s, C₅Me₅), 20.9 (s, CH₃), 36.9 (d, ¹J_{CP} = 35.2 Hz, PCH₂), 100.8 (s, C₅Me₅), 103.5 (dd, ²J_{CP} = 32.2 Hz, ¹J_{CRh} = 54.3 Hz, C_α), 103.6 (d, ³J_{CP} = 7.1 Hz, C_β), 118.2 (d, ³J_{CP} = 11.1 Hz, =CH₂), 126.3-134.2 (Ph and CH=CH₂) ppm; ³¹P {¹H} NMR (121.5 MHz, CD₂Cl₂, 298K) δ = 39.7 (d, ¹J_{RhP} = 127.6 Hz) ppm; IR (KBr): ν = 2099 (m, C≡C) cm⁻¹; elemental analysis calc (%) for C₄₃H₄₄PRh · 1/2 CH₂Cl₂ (737.15): C 70.87, H 6.15; found: C 70.97, H 6.12.

Synthesis of complex [Rh(η⁵-C₅Me₅)(C≡CPh)₂{κ¹-(P)-Ph₂PCH₂CH₂CH=CH₂}] (3a**).** To a solution of the complex [Rh(η⁵-C₅Me₅)Cl₂{κ¹-(P)-Ph₂PCH₂CH₂CH=CH₂}] (200 mg, 0.36 mmol) in THF (20 mL) was added a freshly solution of lithium phenyl acetylide in THF (1.80 mmol, 2.25 mL, 0.8 M) and it was stirred for 15 min at rt. The solution was evaporated to dryness and the solid residue was treated with dichloromethane (25 mL) and filtered. Evaporation of the filtrate and the addition of a

mixture of ether: hexane 1:1 (20 mL) yielded a brown solid. The solvents were decanted and the solid was dried under vacuum. (0.15 g, 60%): ¹H NMR (400.1 MHz, CD₂Cl₂, 298K) δ = 1.63 (d, ⁴J_{HP} = 2.8 Hz, 15H, C₅Me₅), 2.36 (m, 2H, CH₂), 2.93 (m, 2H, PCH₂), 4.83 (m, 1H, =CH₂), 4.93 (m, 1H, =CH₂), 5.81 (m, 1H, CH=CH₂), 7.11 (m, 2H, Ph), 7.22 (m, 4H, Ph), 7.36 (m, 4H, Ph), 7.49 (m, 6H, Ph), 7.87 (m, 4H, Ph) ppm; ¹³C {¹H} NMR (100.6 MHz, CD₂Cl₂, 298K) δ = 8.9 (s, CH₃, C₅Me₅), 28.7 (s, CH₂), 31.0 (d, ¹J_{CP} = 36.2 Hz, PCH₂), 101.4 (m, C₅Me₅), 104.2 (d, ³J_{CP} = 11.1 Hz, C_β), 104.7 (dd, ²J_{CP} = 33.2 Hz, ¹J_{CRh} = 53.3 Hz, C_α), 114.0 (s, =CH₂), 124.5 (s, Ph), 127.8 (s, Ph), 128.0 (d, ²J_{CP} = 10.1 Hz, Ph), 129.3 (s, Ph), 130.3 (s, Ph), 130.8 (s, Ph), 131.4 (d, ¹J_{CP} = 42.0 Hz, Ph), 133.5 (d, ²J_{CP} = 9.1 Hz, Ph), 138.9 (d, ²J_{CP} = 16.1 Hz, CH=CH₂) ppm; ³¹P {¹H} NMR (121.5 MHz, CD₂Cl₂, 298K) δ = 38.4 (d, ¹J_{RhP} = 126.5 Hz) ppm; IR (KBr): ν = 2093 (m, C≡C) cm⁻¹; MS (ESI): *m/z* 703 [M + Na]⁺, 463 [M + Na - HADPP]⁺; elemental analysis calc (%) for C₄₂H₄₂PRh (680.68): C 74.11, H 6.22; found: C 74.13, H 6.22.

Synthesis of the complexes [Rh(η⁵-C₅Me₅)(C≡CR)₂(PPh₂Me)] (R = Ph (4a**), *p*-tol (**4b**)).** To a solution of the complex [Rh(η⁵-C₅Me₅)Cl₂(PPh₂Me)] (200 mg, 0.39 mmol) in THF (20 mL) was added a freshly solution of the correspondent lithium acetylide in THF (1.95 mmol, molar ratio Rh/Li = 1/5). The orange solution was stirred at room temperature for 30 min. Then, the solution was evaporated to dryness and the solid residue was treated with dichloromethane (20 mL) and filtered. Evaporation of the filtrate and addition of hexane (20 mL) yielded a yellow solid. The solvents were decanted and the solid was dried under vacuum. R = Ph (**4a**), (0.17 g, 67%): ¹H NMR (400.1 MHz, CD₂Cl₂, 298K) δ = 1.67 (d, ⁴J_{HP} = 3.0 Hz, 15H, C₅Me₅), 2.30 (d, ²J_{HP} = 11.1 Hz, 3H, PPh₂(CH₃)), 7.06-7.70 (m, 16H, Ph), 7.79-7.89 (m, 4H, Ph) ppm; ¹³C {¹H} NMR (100.6 MHz, CD₂Cl₂, 298K) δ = 9.0 (s, CH₃, C₅Me₅), 18.1 (d, ¹J_{CP} = 42.3 Hz PPh₂(CH₃)), 100.9 (s, C₅Me₅), 103.6 (d, ³J_{CP} = 11.5 Hz, C_β), 105.2 (dd, ²J_{CP} = 31.2 Hz, ¹J_{CRh} = 52.3 Hz, -C_α), 124.5-133.7 (Ph) ppm; ³¹P {¹H} NMR (121.5 MHz, CD₂Cl₂, 298K) δ = 33.0 (d, ¹J_{RhP} = 125.1 Hz) ppm; IR (KBr): ν = 2105 (m, C≡C) cm⁻¹; elemental analysis calc (%) for C₃₉H₃₈PRh (640.61): C 73.12, H 5.98; found: C 73.69, H 6.24. R = *p*-tol (**4b**), (0.15 g, 58%): ¹H NMR (400.1 MHz, CD₂Cl₂, 298K) δ = 1.67 (d, ⁴J_{HP} = 3.1 Hz, 15H, C₅Me₅), 2.29 (d, ²J_{HP} = 11.0 Hz, 3H, PPh₂CH₃), 2.32 (s, 3H, CH₃), 7.03 (d, ³J_{HH} = 7.8 Hz, 2H, *p*-tol), 7.16 (d, ³J_{HH} = 8.0 Hz, 2H, *p*-tol), 7.46 (m, 6H, Ph), 7.83-7.88 (m, 4H, Ph) ppm; ¹³C {¹H} NMR (100.6 MHz, CD₂Cl₂, 298K) δ = 9.0 (s, CH₃, C₅Me₅), 18.2 (d, ¹J_{CP} = 41.2 Hz PPh₂(CH₃)), 22.7 (s, 6H, CH₃, *p*-tol), 100.7 (s, C₅Me₅), 103.2 (d, ³J_{CP} = 8.0 Hz, C_β), 103.3 (dd, ²J_{CP} = 33.2 Hz, ¹J_{CRh} = 54.3 Hz, C_α), 126.3-134.1 (Ph) ppm; ³¹P {¹H} NMR (121.5 MHz, CD₂Cl₂, 298K) δ = 33.1 (d, ¹J_{RhP} = 124.9 Hz) ppm; IR (KBr): ν = 2095 (m, C≡C) cm⁻¹; elemental analysis calc (%) for C₄₁H₄₂PRh · 1/2 CH₂Cl₂ (711.13): C 70.09, H 6.10; found: C 70.86, H 5.91.

Synthesis of the complexes [Rh(η⁵-C₅Me₅)(η³-C(R)CC(=C(R)CH₃))₂{κ¹-(P)-iPr₂PCH₂CH=CH₂}] [CF₃SO₃] (R = Ph (5a**); R = *p*-tol (**5b**)).** To a solution of the correspondent complex [Rh(η⁵-C₅Me₅)(C≡CR)₂{κ¹-(P)-iPr₂PCH₂CH=CH₂}] [100 mg, 0.17 mmol (R = Ph), 0.16 mmol (R = *p*-tol)] in CH₂Cl₂ (10 mL), CH₃OTf [28.5 μL, 0.26 mmol (R = Ph), 43.9 μL, 0.40 mmol (R = *p*-tol)] was added and the resulting solution was stirred for 2.5 h. The solvent was then evaporated. Addition of heptane to the solid residue yielded a brown solid. The solvents were decanted and the solid was dried under vacuum. Complexes **5a,b** are highly higroscopic and analytically pure samples were obtained by anion exchange with NaBPh₄. Thus, to the corresponding complex **5a,b** in CH₂Cl₂ (10 mL), an excess (1: 10) of NaBPh₄ was added. The resulting solution was stirred for 2 h at room temperature and filtered through kieselguhr. The solvent was removed and hexane (20 mL) was added yielding stable BPh₄ salts a brown solids. R = Ph (**5a**), (0.087 g, 67%): ¹H NMR (400.1 MHz, CD₂Cl₂, 298K) δ = 1.07-1.31 (m, 12H, PCH(CH₃)₂), 1.84

(d, $^1J_{HP} = 2.4$ Hz, 15H, C_5Me_5), 2.17-2.27 (m, 4H, $PCH(CH_3)_2$, PCH_2), 2.78 (s, CH_3), 5.01-5.09 (m, 2H, $=CH_2$), 5.61 (m, 1H, $CH=CH_2$), 7.43 (m, 1H, Ph), 7.51-7.58 (m, 5H, Ph), 7.71 (d, $^3J_{HH} = 6.4$ Hz, Ph), 7.82 (d, $^3J_{HH} = 7.6$ Hz, Ph) ppm; ^{13}C { 1H } NMR (100.6 MHz, CD_2Cl_2 , 298K) $\delta = 10.2$ (s, CH_3 , C_5Me_5), 18.3, 18.4, 18.6, 18.9 (4s, $PCH(CH_3)_2$), 23.1 (s, $=C(Ph)CH_3$), 25.2 (d, $^1J_{CP} = 28.2$ Hz, $PCH(CH_3)_2$), 25.7 (d, $^1J_{CP} = 24.1$ Hz, $PCH(CH_3)_2$), 26.5 (d, $^1J_{CP} = 19.1$ Hz, PCH_2), 44.6 (d, $^1J_{CRh} = 4.1$ Hz, C-2), 102.8 (d, $^1J_{CRh} = 4.1$ Hz, C_5Me_5), 109.8 (dd, $^1J_{CRh} = 14.1$ Hz, $^2J_{CP} = 5.0$ Hz, C-1), 119.5 (d, $^3J_{CP} = 10.1$ Hz, $=CH_2$), 120.1 (q, CF_3 , $^1J_{CF} = 318.8$ Hz), 123.9 (s, Ph), 125.6-129.5 (Ph), 130.0 (d, $^2J_{CP} = 10.6$ Hz, $CH=CH_2$), 130.1-132.1 (Ph), 134.8 (s, C-4), 139.6 (s, Ph), 141.6 (dd, $^1J_{CRh} = 23.1$ Hz, $^2J_{CP} = 11.1$ Hz, C-3) ppm; 3P { 1H } NMR (121.5 MHz, CD_2Cl_2 , 298K) $\delta = 39.5$ (d, $^1J_{RHP} = 155.7$ Hz) ppm; IR (nujol): $\nu = 1261$ (s, OTf), 1170 (ms, OTf), 1032 (ms, OTf) cm^{-1} ; conductivity (acetone): $\Lambda = 143$ S \cdot cm 2 \cdot mol $^{-1}$, elemental analysis calc (%) for $C_{60}H_{67}BPRh$ (932.89): C 77.25, H 7.24; found: C 77.32, H 7.55. R = *p*-tol (**5b**), (0.075 g, 58%): 1H NMR (400.1 MHz, CD_2Cl_2 , 298K) $\delta = 0.95$ -1.20 (m, 12H, $PCH(CH_3)_2$), 1.79 (d, $^1J_{HP} = 2.3$ Hz, C_5Me_5), 1.90-2.25 (m, 4H, $PCH(CH_3)_2$, PCH_2), 2.38, 2.46 (2s, 3H, CH_3 , *p*-tol), 2.73 (s, 3H, CH_3), 4.82-5.03 (m, 2H, $=CH_2$), 5.46-5.68 (m, 1H, $CH=CH_2$), 7.33 (d, $^3J_{HH} = 8.1$ Hz, 2H, *p*-tol), 7.37 (d, $^3J_{HH} = 8.0$ Hz, 2H, *p*-tol), 7.59 (d, $^3J_{HH} = 8.0$ Hz, 2H, *p*-tol), 7.73 (d, $^3J_{HH} = 8.2$ Hz, 2H, *p*-tol) ppm; ^{13}C { 1H } NMR (100.6 MHz, CD_2Cl_2 , 298K) $\delta = 10.4$ (s, CH_3 , C_5Me_5), 18.0-18.9 (4s, $PCH(CH_3)_2$), 21.1, 21.6 (2s, CH_3 , *p*-tol), 23.3 (s, $=C(p\text{-tol})CH_3$), 24.8 (d, $^1J_{CP} = 21.1$ Hz, $PCH(CH_3)_2$), 25.5 (d, $^1J_{CP} = 34.2$ Hz, $PCH(CH_3)_2$), 25.7 (d, $^1J_{CP} = 30.1$ Hz, PCH_2), 43.1 (s, C-2), 102.3 (d, $^1J_{CRh} = 4.0$ Hz, C_5Me_5), 109.7 (m, C-1), 120.1 (d, $^3J_{CP} = 10.6$ Hz, $=CH_2$), 120.6 (q, $^1J_{CF} = 314.0$ Hz, CF_3), 125.6-140.7 ($CH=CH_2$ and *p*-tol), 130.9 (s, C-4), 140.6 (dd, $^1J_{CRh} = 21.1$ Hz, $^2J_{CP} = 11.1$ Hz, C-3) ppm; 3P { 1H } NMR (121.5 MHz, CD_2Cl_2 , 298K) $\delta = 39.6$ (d, $^1J_{RHP} = 157.9$ Hz) ppm; IR (nujol): $\nu = 1260$ (s, OTf), 1170 (ms, OTf), 1043 (ms, OTf) cm^{-1} ; conductivity (acetone): $\Lambda = 141$ S \cdot cm 2 \cdot mol $^{-1}$, elemental analysis calc (%) for $C_{62}H_{71}BPRh$ (960.94): C 77.50, H 7.45; found: C 77.27, H 7.70.

Synthesis of the complexes $[Rh(\eta^5-C_5Me_5)\{\eta^3-C(R)CC(=C(R)CH_3)\}\{\kappa^1-(P)-Ph_2PCH_2CH=CH_2\}][CF_3SO_3]$ (R = Ph (6a**), *p*-tol (**6b**)).** CH_3OTf [25.2 μ L, 0.23 mmol (R = Ph), 39.5 μ L, 0.36 mmol (R = *p*-tol)] was added to a solution of the correspondent complex $[Rh(\eta^5-C_5Me_5)(C\equiv CR)_2\{\kappa^1-(P)-Ph_2CH_2CH=CH_2\}]$ [100 mg, 0.15 mmol (R = Ph), 0.14 mmol (R = *p*-tol)] in CH_2Cl_2 (10 mL), and the solution was stirred for 1h and 30 min (**6a**) or 2h and 30 min (**6b**). The solvent was evaporated (ca 2mL) and heptane (20 mL) was added to produce a brown solid precipitate. The solvents were decanted and the solid was dried under vacuum. Analytically pure samples were obtained by anion exchange with $NaBPh_4$ using the procedure described for complexes **5a,b**. R = Ph (**6a**), (0.090 g, 76%): 1H NMR (400.1 MHz, CD_2Cl_2 , 298K) $\delta = 1.64$ (d, $^1J_{HP} = 2.8$ Hz, 15H, C_5Me_5), 2.52-2.67 (m, 4H, CH_3 , PCH_2), 2.79 (m, 1H, PCH_2), 4.68 (m, 1H, $=CH_2$), 4.86 (m, 1H, $=CH_2$), 5.29 (m, 1H, $CH=CH_2$), 7.43-7.61 (m, 20H, Ph) ppm; ^{13}C { 1H } NMR (100.6 MHz, CD_2Cl_2 , 243K) $\delta = 9.3$ (s, CH_3 , C_5Me_5), 22.5 (s, $=C(Ph)CH_3$), 31.1 (d, $^1J_{CP} = 25.1$ Hz, PCH_2), 44.5 (s, C-2), 102.8 (s, C_5Me_5), 109.8 (d, $^1J_{CRh} = 11.1$ Hz, C-1), 120.1 (q, CF_3 , $^1J_{CF} = 318.8$ Hz), 122.8-127.0 (Ph), 128.1 (d, $^2J_{CP} = 10.6$ Hz, $CH=CH_2$), 128.6-134.1 (Ph), 135.0 (s, C-4), 139.1 (Ph), 142.6 (dd, $^1J_{CRh} = 23.1$ Hz, $^2J_{CP} = 9.7$ Hz, C-3) ppm; 3P { 1H } NMR (121.5 MHz, CD_2Cl_2 , 298K) $\delta = 32.9$ (d, $^1J_{RHP} = 162.8$ Hz) ppm; IR (nujol): $\nu = 1259$ (s, OTf), 1158 (ms, OTf), 1030 (ms, OTf) cm^{-1} ; conductivity (acetone): $\Lambda = 138$ S \cdot cm 2 \cdot mol $^{-1}$; elemental analysis calc (%) for $C_{66}H_{63}BPRh\cdot CH_2Cl_2$ (1085.85): C 74.11, H 6.03; found: C 74.85, H 6.29. R = *p*-tol (**6b**), (0.095 g, 79%): 1H NMR (400.1 MHz, CD_2Cl_2 , 298K) $\delta = 1.73$ (d, $^1J_{HP} = 3.1$ Hz, 15H, C_5Me_5), 2.37, 2.44 (2s, 3H, CH_3 , *p*-tol), 2.67 (s, 3H, CH_3), 2.92-2.99 (m, 1H, PCH_2), 3.04-3.10 (m, 1H, PCH_2), 4.71-4.83 (m, 2H, $=CH_2$), 5.19-5.38 (m, 1H, $CH=CH_2$), 7.28-7.62 (m, 18H, Ph and *p*-tol) ppm; ^{13}C { 1H } NMR (100.6 MHz, CD_2Cl_2 , 243K) $\delta = 9.3$ (s, CH_3 , C_5Me_5), 21.1, 21.7 (2s, CH_3 , *p*-tol), 22.7 (s, $=C(p$ -

tol) CH_3), 30.3 (d, $^1J_{CP} = 25.1$ Hz, PCH_2), 43.0 (s, C-2), 102.3 (d, $^1J_{CRh} = 3.5$ Hz, C_5Me_5), 109.1 (dd, $^1J_{CRh} = 12.6$ Hz, $^2J_{CP} = 4.5$ Hz, C-1), 120.4 (q, $^1J_{CF} = 317.9$ Hz, CF_3), 121.1 (d, $^3J_{CP} = 9.1$ Hz, $=CH_2$), 125.6 (s, *p*-tol), 128.2 (d, $^2J_{CP} = 10.6$ Hz, $CH=CH_2$), 128.6-131.9 (Ph and *p*-tol), 132.3 (s, C-4), 133.9-141.4 (Ph and *p*-tol), 141.4 (d, $^1J_{CRh} = 23.0$ Hz, $^2J_{CP} = 11.0$ Hz, C-3) ppm; 3P { 1H } NMR (121.5 MHz, CD_2Cl_2 , 298K) $\delta = 34.3$ (d, $^1J_{RHP} = 162.8$ Hz) ppm; IR (nujol): $\nu = 1250$ (s, OTf), 1168 (ms, OTf), 1031 (ms, OTf) cm^{-1} ; conductivity (acetone): $\Lambda = 140$ S \cdot cm 2 \cdot mol $^{-1}$; elemental analysis calc (%) for $C_{68}H_{67}BPRh\cdot 1/2CH_2Cl_2$ (1071.43): C 76.69, H 6.40; found: C 76.72, H 6.35.

Synthesis of complex $[Rh(\eta^5-C_5Me_5)\{\eta^3-C(Ph)CC(=C(Ph)CH_3)\}\{\kappa^1-(P)-Ph_2PCH_2CH_2CH=CH_2\}][CF_3SO_3]$ (7a**).**

CH_3OTf (40.6 μ L, 0.37 mmol) was added to a solution of complex $[Rh(\eta^5-C_5Me_5)(C\equiv CR)_2\{\kappa^1-(P)-Ph_2CH_2CH_2CH=CH_2\}]$ [(100 mg, 0.15 mmol) in CH_2Cl_2 (10 mL), and the solution was stirred for 105 min. The solvent was evaporated (ca 2mL) and heptane (20 mL) was added to produce a brown solid precipitate. The solvents were decanted and the solid was dried under vacuum. Analytically pure samples were obtained by anion exchange with $NaBPh_4$ using the procedure described for complexes **5a,b**. (0.093 g, 74%): 1H NMR (400.1 MHz, CD_2Cl_2 , 298K) $\delta = 1.58$ (d, $^1J_{HP} = 2.4$ Hz, 15H, C_5Me_5), 1.63-1.91 (m, 3H, CH_2 , PCH_2), 2.46 (m, 3H, CH_3), 3.45 (m, 1H, PCH_2), 4.71 (m, 1H, $=CH_2$), 4.80 (m, 1H, $=CH_2$), 5.49 (m, 1H, $CH=CH_2$), 7.36-7.90 (m, 20H, Ph) ppm; ^{13}C { 1H } NMR (100.6 MHz, CD_2Cl_2 , 298K) $\delta = 9.4$ (s, CH_3 , C_5Me_5), 22.4 (s, $=C(Ph)CH_3$), 23.9 (d, $^1J_{CP} = 25.1$ Hz, PCH_2), 27.5 (d, $^1J_{CP} = 5.0$ Hz, CH_2), 43.8 (s, C-2), 102.5 (d, $^1J_{CRh} = 4.0$ Hz, C_5Me_5), 109.8 (dd, $^1J_{CRh} = 11.8$ Hz, $^2J_{CP} = 3.6$ Hz, C-1), 115.3 (s, $=CH_2$), 120.3 (q, CF_3 , $^1J_{CF} = 318.9$ Hz), 122.8-133.8 (Ph and $CH=CH_2$), 134.3 (s, C-4), 136.6-138.7 (Ph), 142.8 (dd, $^1J_{CRh} = 22.4$ Hz, $^2J_{CP} = 10.9$ Hz, C-3) ppm; 3P { 1H } NMR (121.5 MHz, CD_2Cl_2 , 298K) $\delta = 32.1$ (d, $^1J_{RHP} = 161.6$ Hz) ppm; IR (nujol): $\nu = 1265$ (s, OTf), 1153 (ms, OTf), 1031 (ms OTf) cm^{-1} ; conductivity (acetone): $\Lambda = 143$ S \cdot cm 2 \cdot mol $^{-1}$; E/M (ESI) m/z 695 [M] $^+$; elemental analysis calc (%) for $C_{67}H_{65}BPRh\cdot 1/2CH_2Cl_2$ (1055.39): C 76.82, H 6.11; found: C 76.14, H 5.73.

Synthesis of the complexes $[Rh(\eta^5-C_5Me_5)\{\eta^3-C(R)CC(=C(R)CH_3)\}(PPh_2Me)][CF_3SO_3]$ (R = Ph (8a**), *p*-tol (**8b**)).**

CH_3OTf [41.7 μ L, 0.38 mmol (R = Ph), 40.6 μ L, 0.37 mmol (R = *p*-tol)] was added to a solution of the correspondent complex $[Rh(\eta^5-C_5Me_5)(C\equiv CR)_2(PPh_2Me)]$ [100 mg, 0.16 mmol (R = Ph), 0.15 mmol (R = *p*-tol)] in CH_2Cl_2 (10 mL), and the solution was stirred for 2h. The solvent was then evaporated and the addition of heptane yielded a brown solid. The solvents were decanted and the solid was dried under vacuum. Analytically pure samples were obtained by anion exchange with $NaBPh_4$ using the procedure described for complexes **5a,b**. R = Ph (**8a**), (0.100 g, 78%): 1H NMR (400.1 MHz, CD_2Cl_2 , 298K) $\delta = 1.76$ (d, $^1J_{HP} = 3.1$ Hz, 15H, C_5Me_5), 1.88 (d, $^2J_{HP} = 9.3$ Hz, 3H, $PPh_2(CH_3)$), 2.72 (s, 3H, $-C=C(Ph)(CH_3)$), 7.28-7.51 (m, 20H, Ph) ppm; ^{13}C { 1H } NMR (100.6 MHz, CD_2Cl_2 , 243K) $\delta = 9.8$ (s, CH_3 , C_5Me_5), 13.4 (d, $^1J_{CP} = 33.2$ Hz, $PPh_2(CH_3)$), 22.6 (s, $=C(Ph)CH_3$), 44.6 (s, C-2), 102.4 (d, $^1J_{CRh} = 3.0$ Hz, C_5Me_5), 109.6 (dd, $^1J_{CRh} = 11.7$ Hz, $^2J_{CP} = 3.5$ Hz, C-1), 120.4 (q, $^1J_{CF} = 321.0$ Hz, CF_3), 123.1-132.6 (Ph), 134.2 (s, C-4), 138.8 (Ph), 143.3 (dd, $^1J_{CRh} = 22.4$ Hz, $^2J_{CP} = 10.7$ Hz, C-3) ppm; 3P { 1H } NMR (121.5 MHz, CD_2Cl_2 , 298K) $\delta = 25.7$ (d, $^1J_{RHP} = 160.3$ Hz) ppm; IR (nujol): $\nu = 1248$ (s, OTf), 1181 (ms, OTf), 1036 (ms, OTf) cm^{-1} ; conductivity (acetone): $\Lambda = 122$ S \cdot cm 2 \cdot mol $^{-1}$; E/M (ESI) m/z 655 [M] $^+$; elemental analysis calc (%) for $C_{64}H_{61}BPRh$ (974.88): C 78.85, H 6.31; found: C 78.21, H 6.47. R = *p*-tol (**8b**), (0.070 g, 60%): 1H NMR (400.1 MHz, CD_2Cl_2 , 298K) $\delta = 1.73$ (d, $^1J_{HP} = 4.0$ Hz, 15H, C_5Me_5), 1.83 (d, $^2J_{HP} = 8.0$ Hz, 3H, $PPh_2(CH_3)$), 2.38, 2.45 (2s, 3H, CH_3 , *p*-tol), 2.66 (s, 3H, $-C=C(p\text{-tol})(CH_3)$), 7.19-7.51 (m, 18H, Ph and *p*-tol) ppm; ^{13}C { 1H } NMR (100.6 MHz, CD_2Cl_2 , 243K) $\delta = 9.7$ (s, CH_3 , C_5Me_5), 13.3 (d, $^1J_{CP} = 32.9$ Hz, $PPh_2(CH_3)$), 21.1, 21.6 (2s, CH_3 , *p*-tol), 22.9 (s, $=C(p\text{-tol})CH_3$), 43.7

(s, C-2), 102.2 (s, C₅Me₅), 109.4 (dd, $J_{CRh} = 11.6$ Hz, $J_{CP} = 2.7$ Hz, C-1), 120.5 (q, $J_{CF} = 320.4$ Hz, CF₃), 119.7-132.4 (Ph and *p*-tol), 133.5 (s, C-4), 136.0-141.2 (Ph and *p*-tol), 142.2 (dd, $J_{CRh} = 23.0$ Hz, $J_{CP} = 11.0$ Hz, C-3) ppm; 3P {¹H} NMR (121.5 MHz, CD₂Cl₂, 298K) $\delta = 26.0$ (d, $J_{RHP} = 161.6$ Hz) ppm; IR (nujol): $\nu = 1272$ (s, OTf), 1154 (ms, OTf), 1032 (ms, OTf) cm⁻¹; conductivity (acetone): $\Lambda = 103$ S·cm²·mol⁻¹; E/M (ESI) *m/z* 683 [M]⁺; elemental analysis calc (%) for C₆₄H₆₁BPRh (1002.94): C 79.04, H 6.53; found: C 78.97, H 6.44.

Synthesis of the complexes [Rh(η^5 -C₅Me₅)(η^3 -C(R)CC(=C(R)H))][k⁻-(P)-Ph₂PCH₂CH=CH₂][BF₄] (R = Ph (**9a**), *p*-tol (**9b**)). HBF₄·Et₂O [20.7 μ L, 0.15 mmol (R = Ph), 19.3 μ L, 0.14 mmol (R = *p*-tol)] was added to a dichloromethane (5 mL) solution of the correspondent complex [Rh(η^5 -C₅Me₅)(C≡CR)₂{k⁻-(P)-Ph₂CH₂CH=CH₂}] [100 mg, 0.15 mmol (R = Ph), 0.14 mmol (R = *p*-tol)], and the resulting solution was stirred at rt for 15min (**9a**) or at 248K for 5min (**9b**). The solvent was removed and the oily residue was stirred in heptane yielded a green (**9a**) or brown (**9b**) precipitate. The solvents were decanted and the resulting solid residue washed with heptane (2x 10 mL) and dried under vacuum. R = Ph (**9a**), (0.084 g, 74%): ¹H NMR (400.1 MHz, CD₂Cl₂, 298K) $\delta = 1.57$ (d, $J_{HP} = 2.8$ Hz, 15H, C₅Me₅), 2.20 (m, 1H, PCH₂), 2.64 (m, 1H, PCH₂), 4.65 (m, 1H, =CH₂), 4.76 (m, 1H, =CH₂), 5.11 (m, 1H, CH=CH₂), 7.12 (s, 1H, =C(Ph)H), 7.25-7.90 (m, 20H, Ph) ppm; ¹³C {¹H} NMR (100.6 MHz, CD₂Cl₂, 243K) $\delta = 9.1$ (s, CH₃, C₅Me₅), 30.6 (d, $J_{CP} = 25.1$ Hz, PCH₂), 42.4 (s, C-2), 102.5 (s, C₅Me₅), 117.2 (dd, $J_{CRh} = 14.1$ Hz, $J_{CP} = 4.0$ Hz, C-1), 120.6 (d, $J_{CP} = 9.1$ Hz, =CH₂), 122.8 (s, Ph), 124.7 (s, C-4), 125.4-134.7 (Ph and CH=CH₂), 142.8 (dd, $J_{CRh} = 21.1$ Hz, $J_{CP} = 8.0$ Hz, C-3) ppm; 3P {¹H} NMR (121.5 MHz, CD₂Cl₂, 298K) $\delta = 33.0$ (d, $J_{RHP} = 162.1$ Hz) ppm; IR (KBr): $\nu = 1056$ (s, BF₄) cm⁻¹; conductivity (acetone): $\Lambda = 143$ S·cm²·mol⁻¹; MS (ESI): *m/z* 667 [M]⁺; elemental analysis calc (%) for C₄₁H₄₁BF₄PRh (754.46): C 65.27, H 5.48; found: C 65.44, H 5.95. R = *p*-tol (**9b**), (0.089 g, 81%): ¹H NMR (400.1 MHz, CD₂Cl₂, 298K) $\delta = 1.60$ (d, $J_{HP} = 3.1$ Hz, 15H, C₅Me₅), 2.48, 2.61 (2s, 3H, CH₃ *p*-tol), 2.65-2.94 (m, 2H, PCH₂), 4.57-4.63 (m, 1H, =CH₂), 4.73-4.98 (m, 1H, =CH₂), 5.03-5.18 (m, 1H, CH=CH₂), 7.05 (s, 1H, -C=C(*p*-tol)(H)), 7.33 (d, $J_{HH} = 7.9$ Hz, 2H, *p*-tol), 7.44 (d, $J_{HH} = 8.0$ Hz, 2H, *p*-tol), 7.57-7.67 (m, 14H, Ph and *p*-tol) ppm; ¹³C {¹H} NMR (100.6 MHz, CD₂Cl₂, 243K) $\delta = 9.1$ (s, CH₃, C₅Me₅), 21.4, 21.7 (2s, 3H, CH₃ *p*-tol), 30.4 (d, $J_{CP} = 24.1$ Hz, PCH₂), 41.5 (s, C-2), 102.3 (d, $J_{CRh} = 3.0$ Hz, C₅Me₅), 117.0 (dd, $J_{CRh} = 14.1$ Hz, $J_{CP} = 3.6$ Hz, C-1), 119.7 (Ph), 120.6 (d, $J_{CP} = 10.6$ Hz, =CH₂), 123.8 (s, C-4), 125.4-126.9 (Ph and *p*-tol), 128.2 (d, $J_{CP} = 10.6$ Hz, CH=CH₂), 128.6-139.4 (Ph and *p*-tol), 141.6 (dd, $J_{CRh} = 20.1$ Hz, $J_{CP} = 4.0$ Hz, C-3), 142.0 (*p*-tol) ppm; 3P {¹H} NMR (121.5 MHz, CD₂Cl₂, 298K) $\delta = 33.7$ (d, $J_{RHP} = 162.0$ Hz) ppm; IR (KBr): $\nu = 1052$ (s, BF₄) cm⁻¹; conductivity (acetone): $\Lambda = 135$ S·cm²·mol⁻¹; elemental analysis calc (%) for C₄₃H₄₅BF₄PRh (782.52): C 66.00, H 5.80; found: C 59.50, H 5.54.

Synthesis of the complexes [Rh(η^5 -C₅Me₅)(η^3 -C(R)CC(=C(R)H))](PPh₂Me)][BF₄] (R = Ph (**10a**), *p*-tol (**10b**)). HBF₄·Et₂O (23.9 μ L, 0.16 mmol) was added to a dichloromethane (5 mL) solution of the correspondent complex [Rh(η^5 -C₅Me₅)(C≡CR)₂(PPh₂Me)] [100 mg, 0.16 mmol (R = Ph), 0.15 mmol (R = *p*-tol)], and the resulting solution was stirred at rt for 15min. The solvent was removed and the oily residue was stirred in heptane yielded a green precipitate. The solvents were decanted and the resulting solid residue washed with heptane (2x 10 mL) and dried under vacuum. R = Ph (**10a**), (0.092 g, 79%): ¹H NMR (400.1 MHz, CD₂Cl₂, 298K) $\delta = 1.75$ (d, $J_{HP} = 3.1$ Hz, 15H, C₅Me₅), 1.86 (d, $J_{HP} = 9.3$ Hz, 3H, PPh₂(CH₃)), 7.12 (s, 1H, =C(Ph)H), 7.20-7.70 (m, 20H, Ph) ppm; ¹³C {¹H} NMR (100.6 MHz, CD₂Cl₂, 243K) $\delta = 9.5$ (s, CH₃, C₅Me₅), 12.9 (d, $J_{CP} = 32.2$ Hz, PPh₂(CH₃)), 43.2 (s, C-2), 102.4 (s, C₅Me₅), 118.5 (m, C-1), 123.1 (s, Ph), 124.5 (s, C-4), 126.9-134.8 (Ph), 143.3 (dd, $J_{CRh} = 20.1$ Hz, $J_{CP} = 9.1$ Hz, C-3) ppm; 3P {¹H} NMR (121.5 MHz, CD₂Cl₂, 298K) $\delta = 26.1$

(d, $J_{RHP} = 160.3$ Hz) ppm; IR (KBr): $\nu = 1032$ (s, BF₄) cm⁻¹; conductivity (acetone): $\Lambda = 133$ S·cm²·mol⁻¹; elemental analysis calc (%) for C₃₉H₃₉BF₄PRh (728.42): C 64.31, H 5.40; found: C 65.14, H 5.82. R = *p*-tol (**10b**), (0.093 g, 82%): ¹H NMR (400.1 MHz, CD₂Cl₂, 298K) $\delta = 1.71$ (d, $J_{HP} = 3.2$ Hz, 15H, C₅Me₅), 1.78 (d, $J_{HP} = 9.6$ Hz, 3H, PPh₂(CH₃)), 2.37, 2.48 (2s, 3H, CH₃ *p*-tol), 7.08 (s, 1H, =C(*p*-tol)H), 7.16-7.36 (m, 18H, Ph and *p*-tol) ppm; ¹³C {¹H} NMR (100.6 MHz, CD₂Cl₂, 298K) $\delta = 9.5$ (s, CH₃, C₅Me₅), 12.8 (d, $J_{CP} = 31.2$ Hz, PPh₂(CH₃)), 21.3, 21.7 (2s, CH₃ *p*-tol), 42.4 (s, C-2), 102.2 (s, C₅Me₅), 118.0 (dd, $J_{CRh} = 15.1$ Hz, $J_{CP} = 4.1$ Hz C-1), 120.1 (s, Ph), 123.7 (s, C-4), 126.7-141.7 (Ph), 142.1 (dd, $J_{CRh} = 21.1$ Hz, $J_{CP} = 9.1$ Hz, C-3) ppm; 3P {¹H} NMR (121.5 MHz, CD₂Cl₂, 298K) $\delta = 26.4$ (d, $J_{RHP} = 162.1$ Hz) ppm; IR (KBr): $\nu = 1029$ (f, BF₄) cm⁻¹; conductivity (acetone): $\Lambda = 152$ S·cm²·mol⁻¹; elemental analysis calc (%) for C₄₁H₄₃BF₄PRh · CH₂Cl₂ (841.39): C 59.95, H 5.39; found: C 59.49, H 5.35.

Synthesis of the complexes [Rh(η^5 -C₅Me₅)(k⁻(P,C,C,C)-¹Pr₂PCH₂C(=CH₂)C(CH₂R)C=CR)][BF₄] (R = Ph (**11a**); R = *p*-tol (**11b**)). HBF₄·Et₂O [25.4 μ L, 0.17 mmol (R = Ph), 23.9 μ L, 0.16 mmol (R = *p*-tol)] was added to a dichloromethane (5 mL) solution of the correspondent complex [Rh(η^5 -C₅Me₅)(C≡CR)₂{k⁻(P)-¹Pr₂CH₂CH=CH₂}] [100 mg, 0.17 mmol (R = Ph), 0.16 mmol (R = *p*-tol)], and the resulting solution was stirred at rt for 4h (**11a**); 2h and 30min (**11b**). The solvent was removed and the oily residue was stirred in heptane yielded a brown precipitate. The solvents were decanted and the resulting solid residue washed with heptane (2x 10 mL) and dried under vacuum. R = Ph (**11a**), (0.089 g, 76%): ¹H NMR (400.1 MHz, CD₂Cl₂, 298K) $\delta = 1.13$ -1.37 (m, 12H, PCH(CH₃)₂), 1.85 (d, $J_{HP} = 2.8$ Hz, 15H, C₅Me₅), 1.95 (m, 1H, PCH(CH₃)₂), 2.05 (m, 1H, PCH₂), 2.37 (m, 1H, PCH₂), 2.46 (m, 1H, PCH(CH₃)₂), 3.12 (d, $J_{HH} = 14.4$ Hz, CH₂Ph), 4.00 (d, $J_{HH} = 14.4$ Hz, CH₂Ph), 5.24 (m, 1H, =CH₂), 5.57 (m, 1H, =CH₂), 7.32-7.99 (m, 10H, Ph) ppm; ¹³C {¹H} NMR (100.6 MHz, CD₂Cl₂, 298K) $\delta = 10.1$ (s, C₅Me₅), 17.7 (d, $J_{CP} = 4.2$ Hz, PCH(CH₃)₂), 18.1 (d, $J_{CP} = 6.5$ Hz, PCH(CH₃)₂), 18.3 (d, $J_{CP} = 2.4$ Hz, PCH(CH₃)₂), 18.7 (s, PCH(CH₃)₂), 25.3 (d, $J_{CP} = 24.1$ Hz, C-6), 25.5 (dd, $J_{CP} = 20.1$ Hz, $J_{CRh} = 1.0$ Hz, PCH(CH₃)₂), 30.5 (dd, $J_{CP} = 22.1$ Hz, $J_{CRh} = 1.4$ Hz, PCH(CH₃)₂), 39.7 (s, CH₂Ph), 80.4 (d, $J_{CRh} = 2.0$ Hz, C-2), 83.6 (dd, $J_{CRh} = 8.0$ Hz, $J_{CP} = 2.0$ Hz, C-3), 92.7 (dd, $J_{CRh} = 17.1$ Hz, $J_{CP} = 5.0$ Hz, C-1), 101.3 (dd, $J_{CRh} = 6.0$ Hz, $J_{CP} = 3.0$ Hz, C₅Me₅), 115.8 (d, $J_{CP} = 11.1$ Hz, C-5), 122.8 (s, Ph), 127.6-132.1 (Ph), 138.7 (s, Ph), 142.6 (d, $J_{CP} = 1.0$ Hz, C-4) ppm; 3P {¹H} NMR (121.5 MHz, CD₂Cl₂, 298K) $\delta = 54.1$ (d, $J_{RHP} = 157.3$ Hz) ppm; IR (KBr): $\nu = 1032$ (s, BF₄) cm⁻¹; conductivity (acetone): $\Lambda = 138$ S·cm²·mol⁻¹; MS (ESI): *m/z* 599 [M]⁺; elemental analysis calc (%) for C₃₅H₄₅BF₄PRh (686.43): C 61.24, H 6.61; found: C 59.83, H 6.42. R = *p*-tol (**11b**), (0.068 g, 60%): ¹H NMR (400.1 MHz, CD₂Cl₂, 298K) $\delta = 1.10$ -1.38 (m, 12H, PCH(CH₃)₂), 1.85 (d, $J_{HP} = 2.8$ Hz, 15H, C₅Me₅), 1.86-1.95 (m, 1H, P(CH(CH₃)₂)), 2.07 (m, 1H, PCH₂), 2.34 (m, 1H, PCH₂), 2.40 (s, 3H, CH₃, -C=C(*p*-tol)), 2.41-2.46 (m, 1H, P(CH(CH₃)₂)), 2.48 (s, 3H, CH₃, CH₂ *p*-tol), 3.07 (d, $J_{HH} = 14.4$ Hz, CH₂(*p*-tol)), 3.98 (d, $J_{HH} = 14.4$ Hz, CH₂(*p*-tol)), 5.23 (m, 1H, =CH₂), 5.58 (m, 1H, =CH₂), 7.26 (d, $J_{HH} = 8.0$ Hz, 2H, *p*-tol), 7.39 (d, $J_{HH} = 8.0$ Hz, 2H, *p*-tol), 7.44 (d, $J_{HH} = 8.0$ Hz, 2H, *p*-tol), 7.26 (d, $J_{HH} = 8.0$ Hz, 2H, *p*-tol) ppm; ¹³C {¹H} NMR (100.6 MHz, CD₂Cl₂, 298K) $\delta = 10.1$ (s, CH₃, C₅Me₅), 17.8 (s, PCH(CH₃)₂), 18.1 (d, $J_{CP} = 7.0$ Hz, PCH(CH₃)₂), 18.3 (d, $J_{CP} = 4.0$ Hz, PCH(CH₃)₂), 18.7 (s, PCH(CH₃)₂), 20.7 (s, CH₃, -C=C(*p*-tol)), 21.3 (s, CH₃ *p*-tol), 25.3 (d, $J_{CP} = 24.1$ Hz, C-6), 25.5 (d, $J_{CP} = 19.1$ Hz, P(CH(CH₃)₂)), 30.4 (d, $J_{CP} = 22.1$ Hz, P(CH(CH₃)₂)), 39.4 (s, *p*-tol), 79.5 (s, C-2), 83.7 (d, $J_{CRh} = 7.0$ Hz, C-3), 92.7 (dd, $J_{CRh} = 16.1$ Hz, $J_{CP} = 4.0$ Hz, C-1), 101.3 (d, $J_{CRh} = 3.0$ Hz, C₅Me₅), 115.5 (d, $J_{CP} = 12.1$ Hz, C-5), 119.6 (s, *p*-tol), 127.5-129.4 (*p*-tol), 130.2 (s, *p*-tol), 132.1 (s, *p*-tol), 135.8 (s, *p*-tol), 136.7 (s, *p*-tol), 140.7 (s, ipso *p*-tol, C-CH₃, -C=C(*p*-tol)), 142.9 (s, C-4) ppm; 3P {¹H} NMR (121.5 MHz, CD₂Cl₂, 298K) $\delta = 53.8$ (d, $J_{RHP} = 156.7$ Hz) ppm; IR (KBr): $\nu = 1051$ (s, BF₄) cm⁻¹; conductivity (acetone):

$\Lambda = 134 \text{ S}\cdot\text{cm}^2\cdot\text{mol}^{-1}$; elemental analysis calc (%) for $\text{C}_{37}\text{H}_{49}\text{BF}_4\text{PRh}$ (714.48): C 62.20, H 6.91; found: C 61.82, H 6.73.

Spectroscopic data for complex $[\text{Rh}(\eta^5\text{-C}_5\text{Me}_5)\{\eta^3\text{-C}(\text{Ph})\text{CC}(\text{C}(\text{Ph})\text{H})\}\{\kappa^-\text{(P)}\text{-iPr}_2\text{PCH}_2\text{CH}=\text{CH}_2\}][\text{BF}_4]$ (12a**).** To a solution of the complex $[\text{Rh}(\eta^5\text{-C}_5\text{Me}_5)(\text{C}\equiv\text{CPh})_2\{\kappa^-\text{(P)}\text{-iPr}_2\text{PCH}_2\text{CH}=\text{CH}_2\}]$ (50 mg, 0.08 mmol) in CH_2Cl_2 (3 mL) at 233K, $\text{HBF}_4\cdot\text{Et}_2\text{O}$ (12.7 μL , 0.08 mmol) was added and the solution was stirred for 4h at 253K. To an aliquot of this solution, drops of CD_2Cl_2 were added to record the NMR experiments. ^{13}C { ^1H } NMR (100.6 MHz, CD_2Cl_2 , 243K) $\delta = 9.6$ (s, CH_3 , C_5Me_5), 18.1, 18.6, 18.7, 19.0 (4s, $\text{PCH}(\text{CH}_3)_2$), 24.7 (d, $^1J_{\text{CP}} = 21.5$ Hz, $\text{PCH}(\text{CH}_3)_2$), 25.1 (d, $^1J_{\text{CP}} = 23.1$ Hz, $\text{PCH}(\text{CH}_3)_2$), 26.0 (d, $^1J_{\text{CP}} = 23.2$ Hz, PCH_2), 43.8 (s, C-2), 102.4 (s, C_5Me_5), 118.5 (m, C-1), 119.9 (m, $=\text{CH}_2$), 123.6 (s, C-4), 125.8-135.0 (Ph γ $\text{CH}=\text{CH}_2$), 142.8 (m, C-3) ppm; ^{31}P { ^1H } NMR (121.5 MHz, CD_2Cl_2 , 243K) $\delta = 41.4$ (d, $^1J_{\text{RhP}} = 155.8$ Hz) ppm.

Computational Methods. The potential energy surface for the protonation of dialkynyl rhodium (III) complexes and their evolution into the η^3 -dienyl or the rhodaphosphacycle complexes was studied with the Density Functional theory, using the B3LYP hybrid functional. The 6-31G* basis set was employed for C, H, P, B, and F atoms, and the LANL2DZ for Rh.¹⁷

The election of the Density Functional theory¹⁹ and the B3LYP functional has been dictated in an attempt to get a compromise between a reasonable view of the energies and geometries of the stationary points of the potential-energy surface of the reactions studied and the requirement of a realistic description of the molecules involved. In this regard, and despite that at this level of theory and working with transition metal complexes, the activation barriers could not be evaluated with a high precision, the semi-quantitative picture emerging from these calculations could be considered as basically correct.^{19, 20}

All stationary points located were fully optimized and characterized to be a minimum or a first-order saddle point (transition structure) by computing the harmonic vibrational frequencies. The connection of either, the reactants or products with a transition state was established by computation of the intrinsic reaction coordinate (IRC). The reaction Gibbs free-energies, ΔG_{rxn} , are referred to the corresponding starting system, and the activation Gibbs free-energy of each step, ΔG^\ddagger is relative to the minimum previous to the corresponding transition state. In all cases, the energies are in kcal mol⁻¹.

All the calculations described in this work were carried out with the Gaussian 09 package.²¹ Geometrical details and the values of the computed Gibbs free-energies of the stationary points located are collected in the Supporting Information section.

X-Ray Crystal Structure Determination of Complexes **5a and **11a**.** All single crystals appropriate for X-ray analysis were obtained using liquid diffusion techniques from dichloromethane/heptane solvent systems. The details of all X-ray single-crystal diffraction experiments are given in Table S1 in the Supporting Information, and molecular structures are shown in Figures 1 and 2. In both cases, diffraction data were recorded on a Oxford Diffraction Xcalibur Nova (Agilent) single crystal diffractometer, at 123 K (for **5a**) and 150 K (for **11a**) using Cu-K α radiation ($\lambda = 1.5418 \text{ \AA}$). Images were collected at a 65 mm fixed crystal-detector distance, using the oscillation method, with 1° oscillation and variable exposure time per image. Data collection strategy was calculated with the program CrysAlis Pro CCD.²² Data reduction and cell refinement was performed with the program CrysAlis Pro RED.²² An empirical absorption correction was applied using the SCALE3 ABSPACK algorithm as implemented in the program CrysAlis Pro RED.²² The software package WINGX²³ was used for space group determination, structure solution and refinement. The structures of the complexes were solved by Patterson interpretation and phase expansion using

DIRDIF²⁴ In **11a**, the asymmetric unit contains two formula units. In one unit, the chain in the rhodaphosphacycle is disordered in two positions with an occupancy factor of 0.5. Isotropic least-squares refinement on F₂ using SHELXL2013²⁵ was performed. During the final stages of the refinements, all the positional parameters and the anisotropic temperature factors of all the non-H atoms were refined and the H atoms were geometrically located and their coordinates were refined riding on their parent atoms. The maximum residual electron density is located near to heavy atoms. The function minimized was $[\sum w(F_o^2 - F_c^2)/\sum w(F_o^2)]^{1/2}$ where $w = 1/[\sigma^2(F_o^2) + (aP)^2 + bP]$ (a and b values are collected in Table S1) from counting statistics and $P = (\text{Max}(F_o^2, 0) + 2F_c^2)/3$. Atomic scattering factors were taken from the International Tables for X-Ray Crystallography International.²⁶ The crystallographic plots were made with PLATON.²⁷ CCDC 1453133-1453134 contains the supplementary crystallographic data for this paper. The data can be obtained free of charge from The Cambridge Crystallographic Data Centre via www.ccdc.cam.ac.uk/structures.

ASSOCIATED CONTENT

Supporting Information

Experimental procedures and characterization data for complexes **1c-d**, **8a-b** and **2c-d**. ^1H and $^{31}\text{P}\{^1\text{H}\}$ NMR Spectra for complexes **1a-d**, **5a**, **9a** and **11a**, and $^1\text{H}\{^{31}\text{P}\}$ for complex **11a**. Crystal data and structure refinement for compounds **5a** and **11a**. Geometrical details (including Figures S16-S22), cartesian coordinates, and the values of the computed Gibbs free-energies of the stationary points located, are collected in the Supporting Information section which includes a reaction energy profile. This material is available free of charge via the Internet at <http://pubs.acs.org>.

AUTHOR INFORMATION

Corresponding Author

* Elena Lastra. Departamento de Química Orgánica e Inorgánica. Universidad de Oviedo. Julian Claveria, 8, 33006 Oviedo, Spain.

E-mail: elb@uniovi.es

Notes

The authors declare no competing financial interest.

ACKNOWLEDGMENT

This work was supported by the Spanish Ministerio de Ciencia e Innovación (CTQ2011-28641) and Consolider Ingenio 2010 (CSD2007-00006). S. Martínez de Salinas thanks the Spanish Ministerio de Educación, Cultura y Deporte for a scholarship.

REFERENCES

- (i) For recent reviews see: a) Trost, B. M.; Li, C.-J. *Modern Alkyne Chemistry: Catalytic and Atom-Economic Transformations*, Wiley-VCH: Weinheim, Germany, **2015**; b) Trost, B. M.; McClory, A. *Chem. Asian J.* **2008**, *3*, 164-194; c) Wiedemann, S. H.; Lee, C. Rhodium and Group 9-11 Metal Vinylidenes in Catalysis. In *Metal Vinylidenes and Allenylidenes in Catalysis*, Wiley-VCH: Weinheim, Germany, **2008**; p 279; d) Bruneau, C.; Dixneuf, P. H. *Angew. Chem. Int. Ed.* **2006**, *45*, 2176-2203; e) Trost, B. M.;

Frederiksen, M. U.; Rudd, M. T. *Angew. Chem. Int. Ed.* **2005**, *44*, 6630-6666.

(2) For recent examples see: a) Boone, M. P.; Stephan, D. W. *Organometallics* **2014**, *33*, 387-393; b) Paredes, P.; Vega, E.; Díez, J.; Gamasa, M. P. *Organometallics* **2012**, *31*, 3798-3801; c) Shi, W.; Liu, C.; Lei, A. *Chem. Soc. Rev.* **2011**, *40*, 2761-2776; d) Shao, Z.; Peng, F. *Angew. Chem. Int. Ed.* **2010**, *49*, 9566-9568; e) Chin, C. S.; Won, G.; Chong, D.; Kim, M.; Lee, H. *Acc. Chem. Res.* **2002**, *35*, 218-225; f) Ohmura, T.; Yorozuya, S.; Yamamoto, Y.; Miyauro, N. *Organometallics* **2000**, *19*, 365-367; g) Older, C. M.; Stryker, J. M. *J. Am. Chem. Soc.* **2000**, *122*, 2784-2797; h) Ohmura, T.; Yamamoto, Y.; Miyauro, N. *J. Am. Chem. Soc.* **2000**, *122*, 4990-4991; i) Takahashi, T.; Tsai, F.-Y.; Kotora, M. *J. Am. Chem. Soc.* **2000**, *122*, 4994-4995; j) Trost, B. M.; Brown, R. E.; Toste, F. D. *J. Am. Chem. Soc.* **2000**, *122*, 5877-5878; k) Trost, B. M.; Toste, J. *J. Am. Chem. Soc.* **2000**, *122*, 714-715; l) Jeong, N.; Sung, B. K.; Choi, Y. K. *J. Am. Chem. Soc.* **2000**, *122*, 6771-6772; m) Waters, M. L.; Bos, M. E.; Wulff, W. D. *J. Am. Chem. Soc.* **1999**, *121*, 6403; n) Kishimoto, Y.; Eckerle, P.; Miyatake, T.; Kainosho, M.; Ono, A.; Ikariya, T.; Noyori, R. *J. Am. Chem. Soc.* **1999**, *121*, 12035. o) Dzwiniel, T. L.; Etkin, N.; Stryker, J. M. *J. Am. Chem. Soc.* **1999**, *121*, 10640.

(3) a) Werner, H. *Coord. Chem. Rev.* **2004**, *248*, 1693-1702; b) Becker, E.; Mereiter, K.; Puchberger, M.; Schmid, R.; Kirchner, K. *Organometallics* **2003**, *22*, 2124-2133; c) Pavlik, S.; Mereiter, K.; Schmid, R.; Kirchner, K. *Organometallics* **2003**, *22*, 1771-1774; d) Becker, E.; Mereiter, K.; Puchberger, M.; Schmid, R.; Kirchner, K.; Doppiu, A.; Salzer, A. *Organometallics* **2003**, *22*, 3164-3170

(4) a) Slugovc, C.; Mereiter, K.; Schmid, R.; Kirchner, K. *Organometallics* **1999**, *18*, 1011-1017; b) Slugovc, C.; Mereiter, K.; Schmid, R.; Kirchner, K. *J. Am. Chem. Soc.* **1998**, *120*, 6175-6176.

(5) Díez, J.; Gamasa, M. P.; Lastra, E.; Villar, A.; Pérez-Carreño, E. *Organometallics* **2007**, *26*, 5315-5322.

(6) a) Baya, M.; Buil, M. L.; Esteruelas, M. A.; Oñate, E. *Organometallics* **2005**, *24*, 2030-2038; b) Baya, M.; Buil, M. L.; Esteruelas, M. A.; Oñate, E. *Organometallics* **2005**, *24*, 5180-5183; c) Baya, M.; Esteruelas, M. A.; Gonzalez, A. I.; López, A. M.; Oñate, E. *Organometallics* **2005**, *24*, 1225-1232.

(7) a) Díez, J.; Gamasa, M. P.; Gimeno, J.; Lastra, E.; Villar, A. *Organometallics* **2005**, *24*, 1410-1418; b) Bassetti, M.; Álvarez, P.; Gimeno, J.; Lastra, E. *Organometallics* **2004**, *23*, 5127-5134; c) Álvarez, P.; Lastra, E.; Gimeno, J.; Bassetti, M.; Falvello, L. R. *J. Am. Chem. Soc.* **2003**, *125*, 2386-2387.

(8) Barthel-Rosa, L. P.; Catalano, V. J.; Maitra, K.; Nelson, J. H. *Organometallics* **1996**, *15*, 3924-3934.

(9) Sánchez-Sordo, I.; Martínez de Salinas, S.; Díez, J.; Lastra, E.; Gamasa, M. P. *Organometallics* **2015**, *34*, 4581-4590.

(10) Jones, W. D.; Kuykendall, V. L. *Inorg. Chem.* **1991**, *30*, 2615-2622.

(11) Since the reactivity observed for complexes **1c,d** and **2c,d** was unsatisfactory, the synthesis of the complexes bearing the phosphanes HADPP and PMe₃Ph and the alkynyls R¹ = SiMe₃ and CH₂Ph have not been attempted. Experimental and spectroscopic data for complexes **1c-d** and **2c-d** can be found in the Supporting Information.

(12) Complexes **1c** and **2c** containing the SiMe₃ group were isolated as oils and their elemental analyses were not satisfactory. ¹H and ³¹P{¹H} NMR spectra for these complexes can be found in the Supporting Information.

(13) a) Field, L. D.; Magill, A. M.; Pike, S. R.; Turnbull, A. J.; Dalgarno, S. C.; Turner, P.; Willis, A. C. *Eur. J. Inorg. Chem.* **2010**, 2406-2414; b) Lynam, J. M.; Nixon, T. D.; Whitwood, A. C. *J. Organomet. Chem.* **2008**, *693*, 3103-3110; c) Bianchini, C.; Bohanna, C.; Esteruelas, M. A.; Frediani, P.; Meli, A.; Oro, L. A.; Peruzzini, M. *Organometallics* **1992**, *11*, 3837-3844; d) Jia, G.; Gallucci, J. C.; Rheingold, A. L.; Haggerty, B. S.; Meek, D. W. *Organometallics* **1991**, *10*, 3459-3465.

(14) a) f) Bianchini, C.; Innocenti, P.; Peruzzini, M.; Romerosa, A.; Zanobini, F. *Organometallics* **1996**, *15*, 272-285; b) Albertin, G.; Antoniutti, S.; Bordignon, E.; Cazzaro, F.; Ianelli, S.; Pelizzi, G. *Organometallics* **1995**, *14*, 4114-4125; c) Bianchini, C.; Peruzzini, M.; Zanobini, F.; Frediani, P.; Albinati, A. *J. Am. Chem. Soc.* **1991**, *113*, 5453-5454; d) Jia, G.; Meek, D. W. *Organometallics* **1991**, *10*, 1444-1450; e) Jia, G.; Gallucci, J. C.; Rheingold, A. L.; Haggerty, B. S.; Meek, D. W. *Organometallics* **1991**, *10*, 3459-3465; f) Jia, G.; Rheingold, A. L.; Meek, D. W. *Organometallics* **1989**, *8*, 1378-1380.

(15) a) Jacques, J.; Collet, A.; Wilen, S. H. *Enantiomers, Racemates and Resolutions* Krieger Publishing Company, Malabar, FL, 1994; b) Pérez-García, L.; Amabilino, D. B. *Chem. Soc. Rev.* **2007**, *36*, 941-967; Gladiali, S. C. *R. Chimie* **2007**, *10*, 220-23; c) Sun, Q.; Bai, Y.; He, G.; Duan, C.; Lin, Z.; Meng, Q. *Chem. Commun.* **2006**, 2777-2779; d) Pérez-García, L.; Amabilino, D. B. *Chem. Soc. Rev.* **2002**, *31*, 342-356.

(16) Stable square planar alkynyl-vinylidene rhodium complexes have been previously reported: a) Schäfer, M.; Wolf, J.; Werner, H. *Dalton Trans.* **2005**, 1468-1481; b) Schäfer, M.; Mahr, N.; Wolf, J.; Werner, H. *Angew. Chem. Int. Ed. Engl.* **1993**, *32*, 1315-1318.

(17) An excellent description of the theoretical methodology, can be found in: F. Jensen, *Introduction to Computational Chemistry*, 2nd edition, Wiley 2007.

(18) Díez, J.; Gamasa, M. P.; Gimeno, J.; Lastra, E.; Villar, A. *J. Organomet. Chem.* **2006**, *691*, 4092-4099.

(19) Cohen, A. J.; Mori-Sánchez, P.; Yang, W. *Chem. Rev.* **2012**, *112*, 289-320.

(20) For a revision of the performance of different functionals used in molecular calculations, see: a) Goerik, L.; Grimme, S. *Phys. Chem. Chem. Phys.*, **2011**, *13*, 6670-6688; b) Rappoport, D.; Crawford, N. R. M.; Furche, F.; Burke, K. Approximate Density Functionals: Which Should I Choose, in "Solomon, E. I., King, R. B., Scott, R. A. (eds.), Computational Inorganic and Bioinorganic Chemistry; 2013. Wiley.

(21) Gaussian 09, Revision B.01, Frisch, M. J.; Trucks, G. W.; Schlegel, H. B.; Scuseria, G. E.; Robb, M. A.; Cheeseman, J. R.; Scalmani, G.; Barone, V.; Mennucci, G.; Petersson, A.; Nakatsuji, H.; Caricato, M.; Li, X.; Hratchian, B.; Izmaylov, A. F.; Bloino, J.; Zheng, G.; Sonnenberg, J. L.; Hada, M.; Ehara, M.; Toyota, K.; Fukuda, R.; Hasegawa, J.; Ishida, M.; Nakajima, T.; Honda, Y.; Kitao, O.; Nakai, H.; Vreven, T.; Montgomery, Jr. J. A.; Peralta, J. E.; Ogliaro, F.; Bearpark, M.; Heyd, J. J.; Brothers, E.; Kudin, K. N.; Staroverov, V. N.; Keith, T.; Kobayashi, R.; Normand, J.; Raghavachari, K.; Rendell, A.; Burant, J. C.; Iyengar, S. S.; Tomasi, J.; Cossi, M.; Rega, N.; Millam, J. M.; Klene, M.; Knox, J. E.; Cross, J. B.; Bakken, V.; Adamo, C.; Jaramillo, J.; Gomperts, R.; Stratmann, R. E.; Yazyev, O.; Austin, A. J.; Cammi, R.; Pomelli, C.; Ochterski, J. W.; Martin, R. L.; Morokuma, K.; Zakrzewski, V. G.; Voth, G. A.; Salvador, P.; Dannenberg, J. J.; Dapprich, S.; Daniels, A. D.; Farkas, O.; Foresman, J. B.; Ortiz, J. V.; Cioslowski, J. and Fox, D. J. Gaussian, Inc., Wallingford CT, 2010.

(22) CrysAlisPro CCD, CrysAlisPro RED. Oxford Diffraction Ltd., Abingdon, Oxfordshire, UK. (2008).

(23) Farrugia L. J. *J. Appl. Crystallogr.* **2012**, *45*, 849-854.

(24) Beurskens, P. T.; Beurskens, G.; de Gelder, R.; Smits, J. M. M.; García-Granda, S.; Gould, R. O.; Smykalla, C. *The DIRDIF Program System*; Technical Report of the Crystallographic Laboratory; University of Nijmegen: Nijmegen, The Netherlands, 2008. Window GUI L. J. Farrugia.

(25) Sheldrick G. M. *SHELXL2013: Program for the Refinement of Crystal Structures*; University of Göttingen: Göttingen, Germany, 2014.

(26) *Tables for X-Ray Crystallography*; Kynoch Press; Birmingham, U.K., 1974; Vol. IV (present distributor: Kluwer Academic Publishers; Dordrecht, The Netherlands).

Table of Contents artwork

